科技醫療應用與安全

Cheng-Ta Huang
Assistant Professor
Department of Information Management,
Yuan Ze University
2020/09/14

NATIONAL CHENGCHI UNIVERSITY

Yuan Ze University

主要研究領域

- 醫學影像
- 影像辨識與分割
- 物件追蹤
- 多媒體資訊安全
- 科技醫療

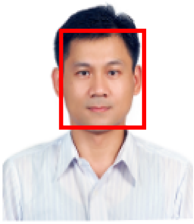

姓名：左瑞麟
職稱：副教授(系主任)
校內分機::62328
raylin@cs.nccu.edu.tw
日本筑波大學 系統與資訊工程博士

研究領域：密碼學、資訊安全、網路安全、區塊鏈與隱私強化技術

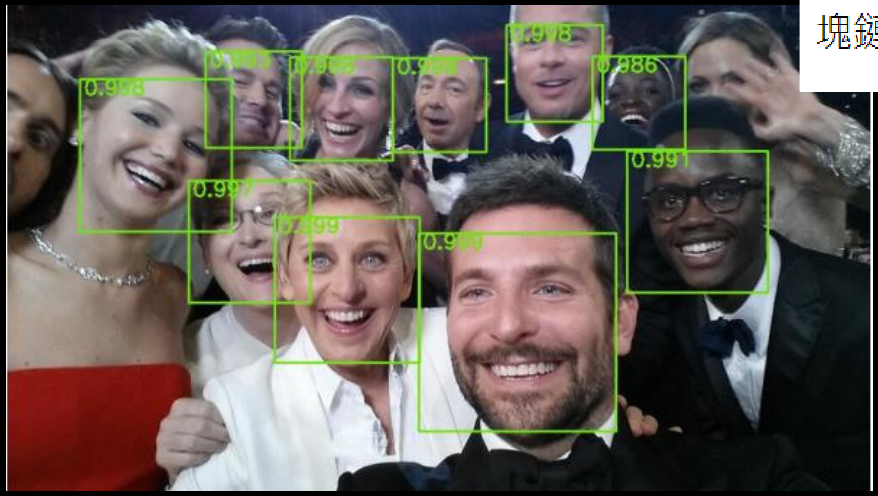

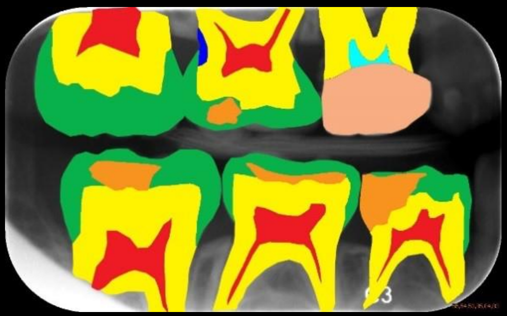

secret data:
“I LOVE NCCU”

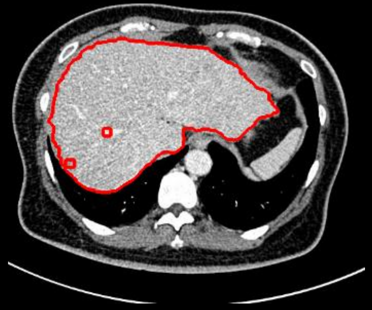

科技醫療應用與安全

- 醫學影像
- 資訊科技
- 影像上的資訊安全

醫學影像

全口 X-ray

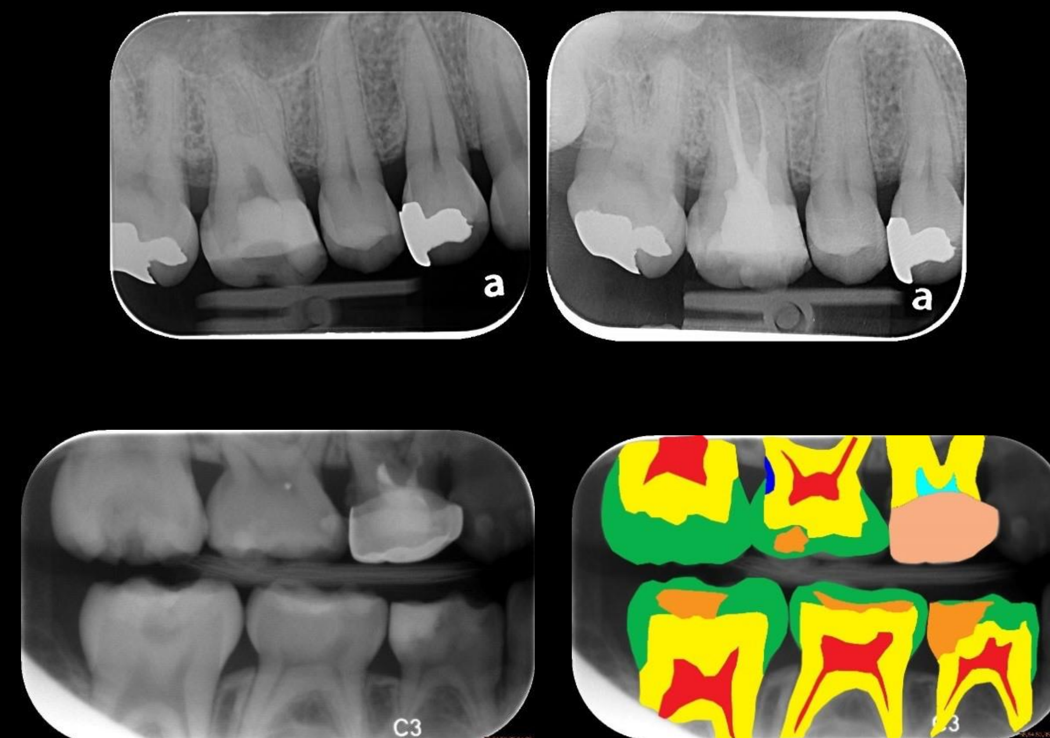

bitewing radiography

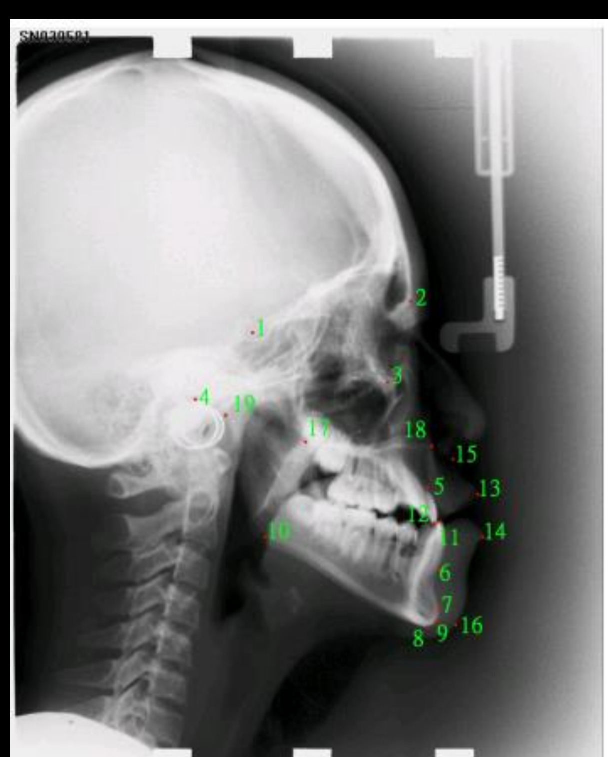

cephalometric X-ray

醫學影像

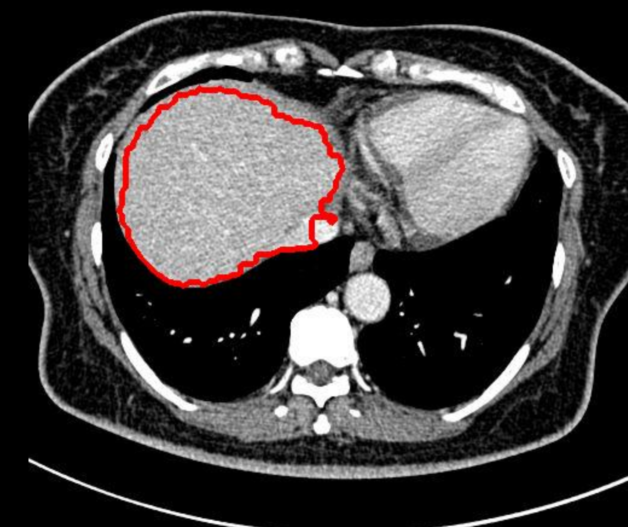

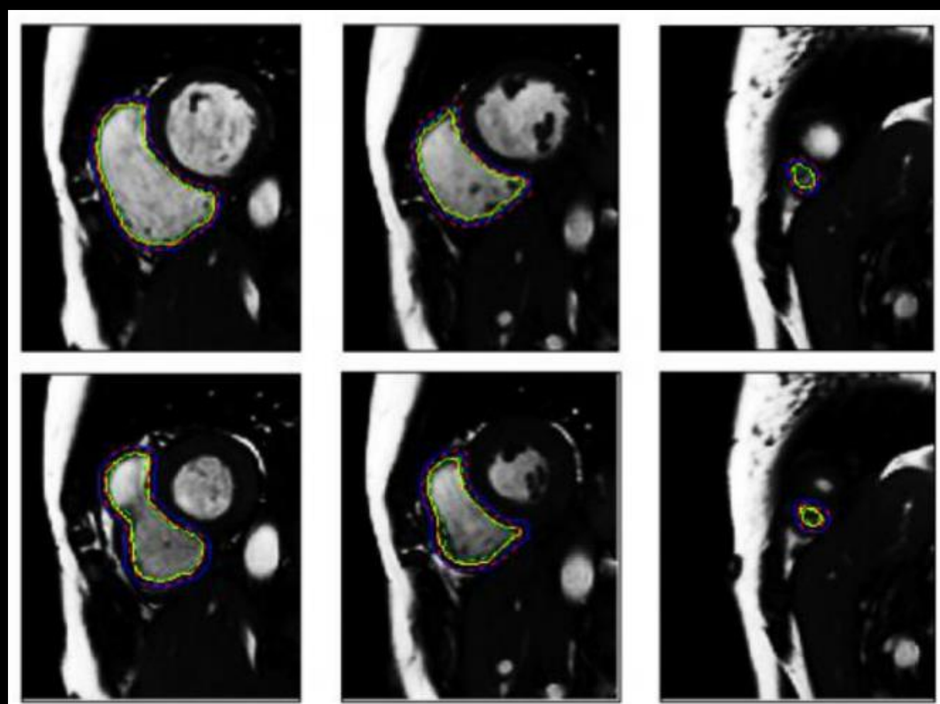

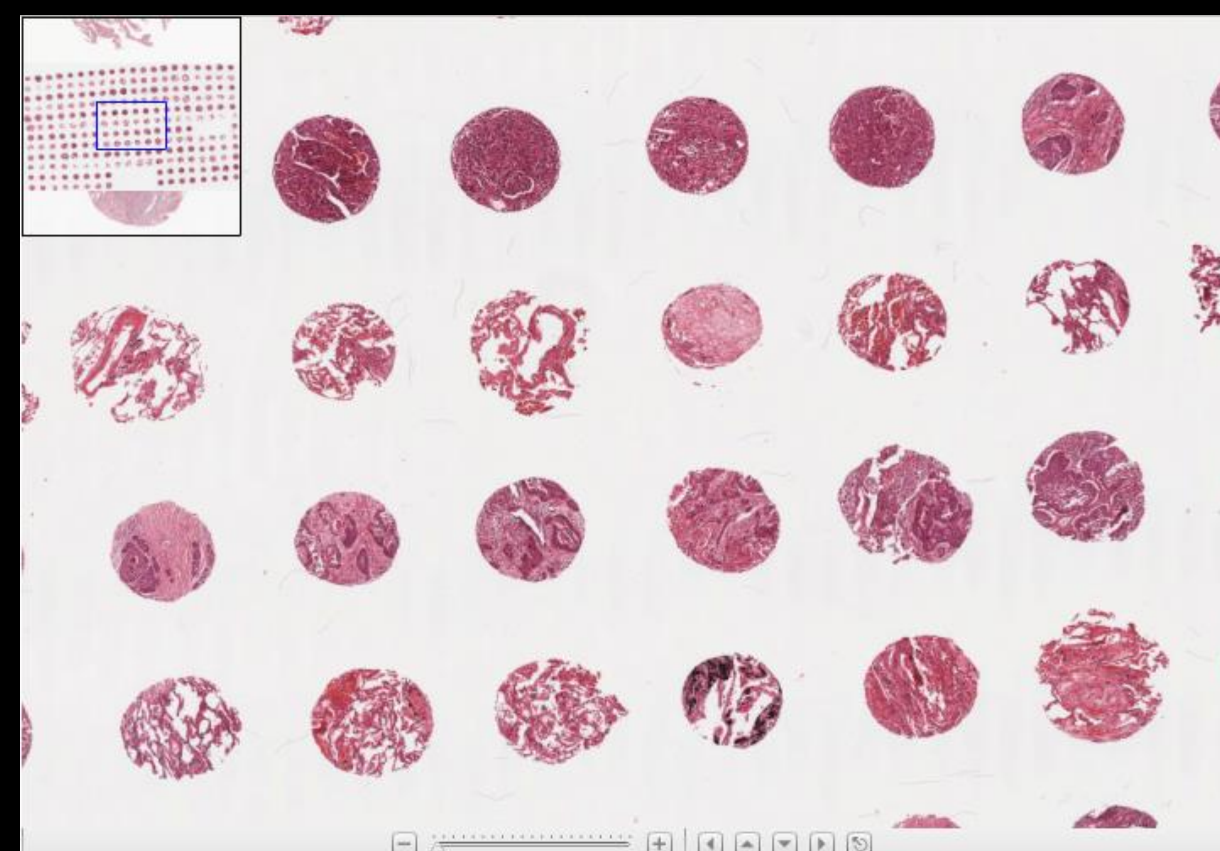

Publication

1. Lindner C., Wang C, **Huang C**., Li C., Chang S., Cootes T.(2016) Fully Automatic System for Accurate Localisation and Analysis of Cephalometric Landmarks in Lateral Cephalograms, Nature-Scientific Reports 6: 33581 **(SCI, JCR 2015 (7/63) in MULTIDISCIPLINARY SCIENCES, IF=5.228)**

2. Wang CW*, **Huang C.**, Lee J., Li C., Chang S., Siao M., Lai T., Ibragimov B., Vrtovec T., Ronnerberger O., Fischer P., Cootes T., Lindner C. (2016) A benchmark for comparison of dental radiography analysis algorithms, Medical Image Analysis 31, 63-76 **(SCI, JCR 2015 (4/104) in COMPUTER SCIENCE, INTERDISCIPLINARY APPLICATIONS, IF=4.565)**

3. Wang C.-W.*, **Huang C.**, Hung C. (2015) VirtualMicroscopy: ultra-fast interactive microscopy of gigapixel / terapixel images over internet, Nature-Scientific Reports 5: 14069 **(SCI, JCR 2015 (7/63) in MULTIDISCIPLINARY SCIENCES, IF=5.228)**

4. Wang C.-W.*, **Huang C.-T.**, Hsieh, M.-C., Li C.H., Chang S.W., Li W.C., Vandaele R, Maree R., Jodogne S., Geurts P., Chen C., Zheng G., Chu C., Mirzaalian H., Hamarneh G., Vrtovec T., Ibragimov B. (2015) Evaluation and Comparison of Anatomical Landmark Detection Methods for Cephalometric X-Ray Images: A Grand Challenge, IEEE Transactions on Medical Imaging 34(9) 1-11 **(SCI, JCR 2015 (9/104) in COMPUTER SCIENCE, INTERDISCIPLINARY APPLICATIONS, IF=3.756)**

醫學影像處理技術

全自動 X-ray 側顱影像分析

- The International Symposium on Biomedical Imaging (ISBI)
  - ISBI 2015, NewYork, USA

  - ISBI 2014, Beijing, China

Cephalogram annotation example showing the 19 landmark positions

1	sella turcica
2	nasion
3	orbitale
4	porion
5	subspinale
6	supramentale
7	pogonion
8	menton
9	gnathion
10	gonion
11	lower incisal incision
12	upper incisal incision
13	upper lip
14	lower lip
15	subnasale
16	soft tissue pogonion
17	posterior nasal spine

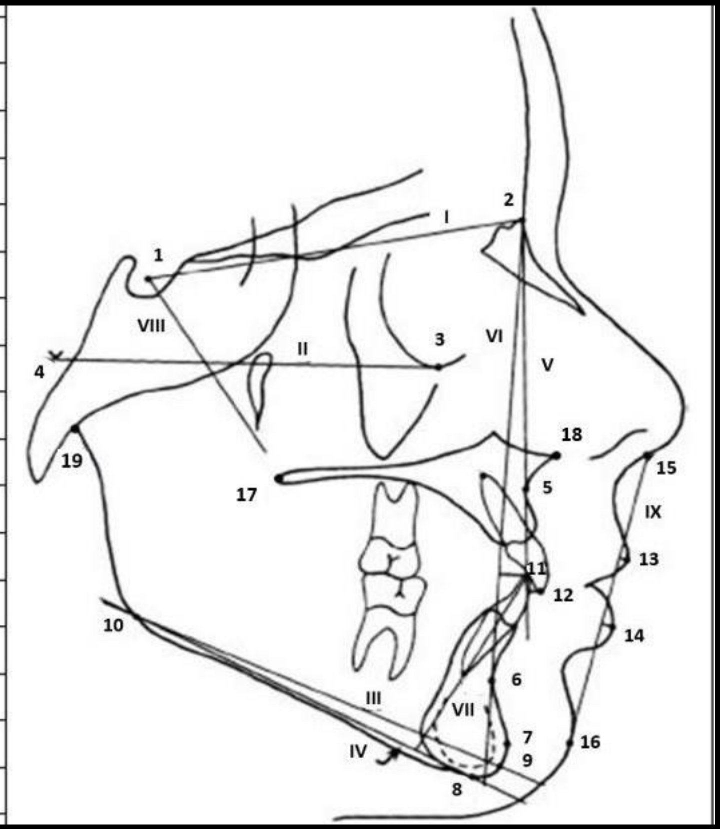

Cephalogram annotation example showing the 19 landmark positions

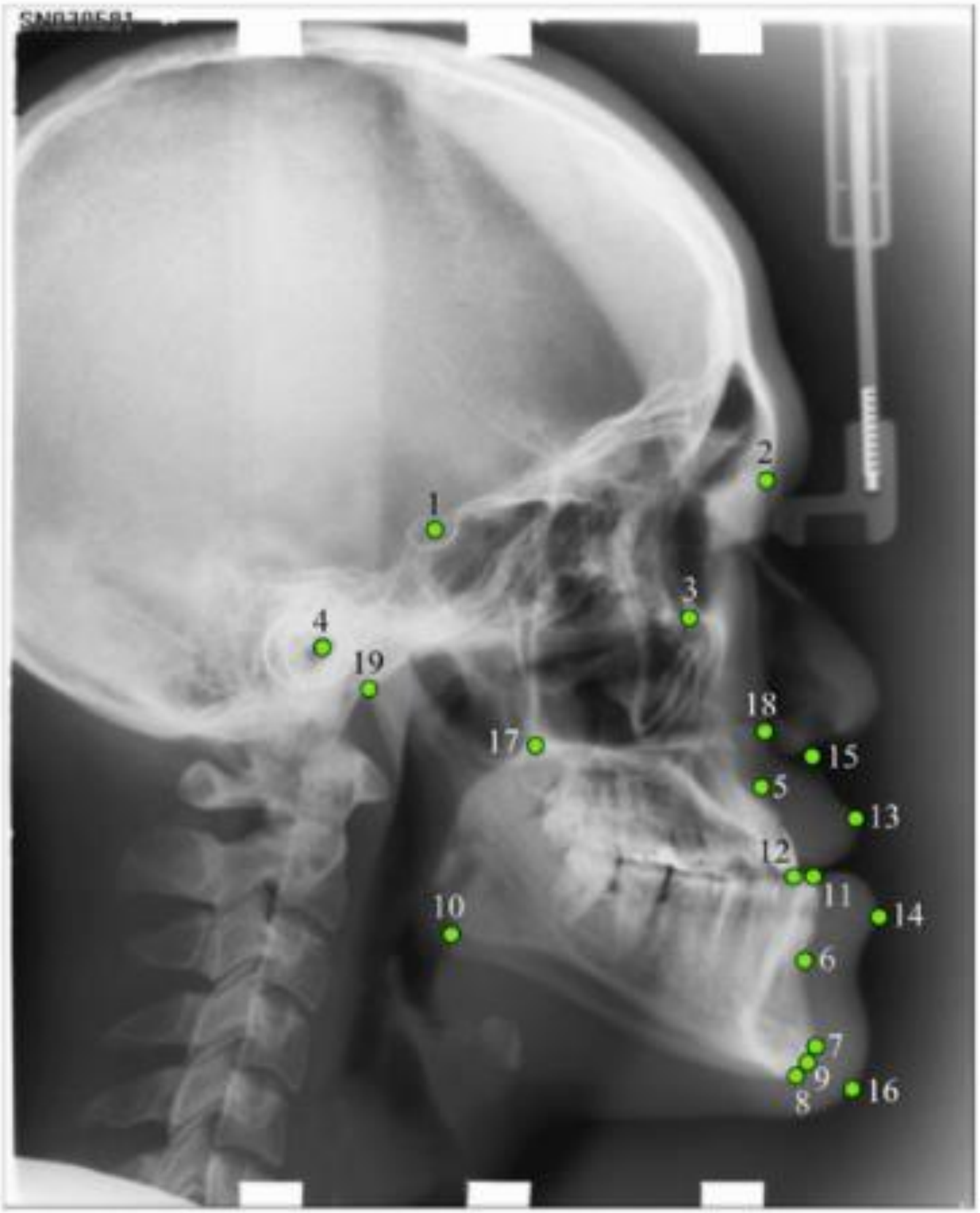

L1	Sella
L2	Nasion
L3	Orbitale
L4	Porion
L5	Subspinale
L6	Supramentale
L7	Pogonion
L8	Menton
L9	Gnathion
L10	Gonion
L11	Incision inferius
L12	Incision superius
L13	Upper lip
L14	Lower lip
L15	Subnasale
L16	Soft tissue pogonion
L17	Posterior nasal spine
L18	Anterior nasal spine
L19	Articulare

Methods	(1) ANB	(2) SNB	(3) SNA	(4) ODI[*1]	(5) APDI[*2]	(6) FHI	(7) FMA	(8) MW
Type 1	3.2°~5.7° Class I (Normal)	74.6°~78.7° Normal mandible	79.4°~83.2° Normal maxilla	Normal: 74.5° ± 6.07	Normal : 81.4° ± 3.8°	Normal : 0.65~0.75	Normal : 26.8°~31.4°	Type 1: Normal : 2mm~4.5mm
Type 2	>5.7° Class II	<74.6° Retrognathic mandible	>83.2° Prognathic maxilla	>80.5° Deep bite tendency	<77.6° Class II tendency	>0.75 Short face tendency	>31.4° Mandible high angle tendency	Type 2: MW=0mm Edge to edge Type 3: MW<0mm Anterior cross bite
Type 3	<3.2° Class III	>78.7° Prognathic mandible	<79.4° Retrognathic maxilla	<68.4° Open bite tendency	>85.2° Class III tendency	<0.65 Long face tendency	<26.8° Mandible lower angle tendency	Type 4: MW>4.5 Large over jet

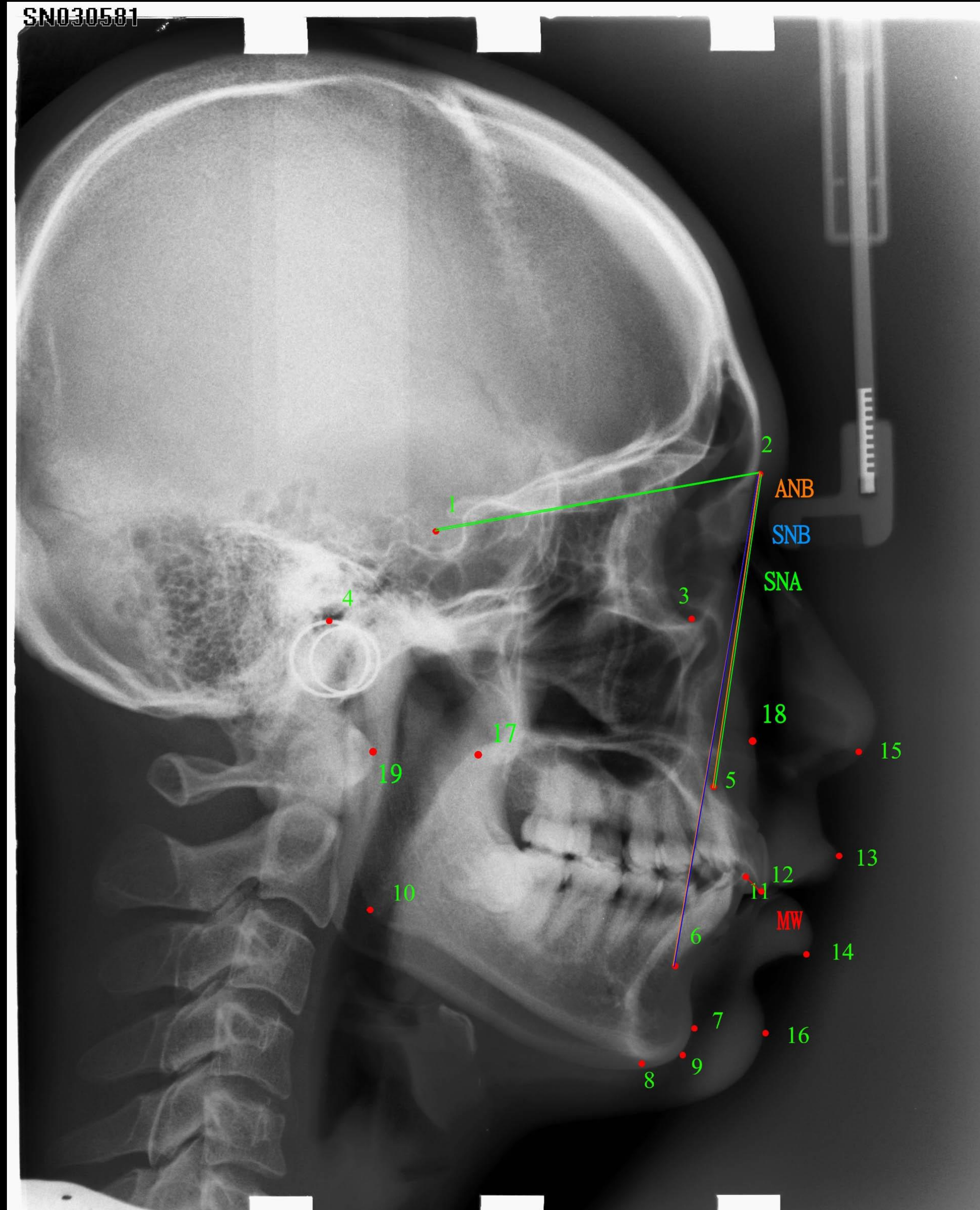
SN030581
1
2
ANB
SNB
SNA
3
4
18
17
15
19
5
13
12
11
10
MW
6
14
7
16
9
8

ODI is 73 degrees (76°-3°=73°)

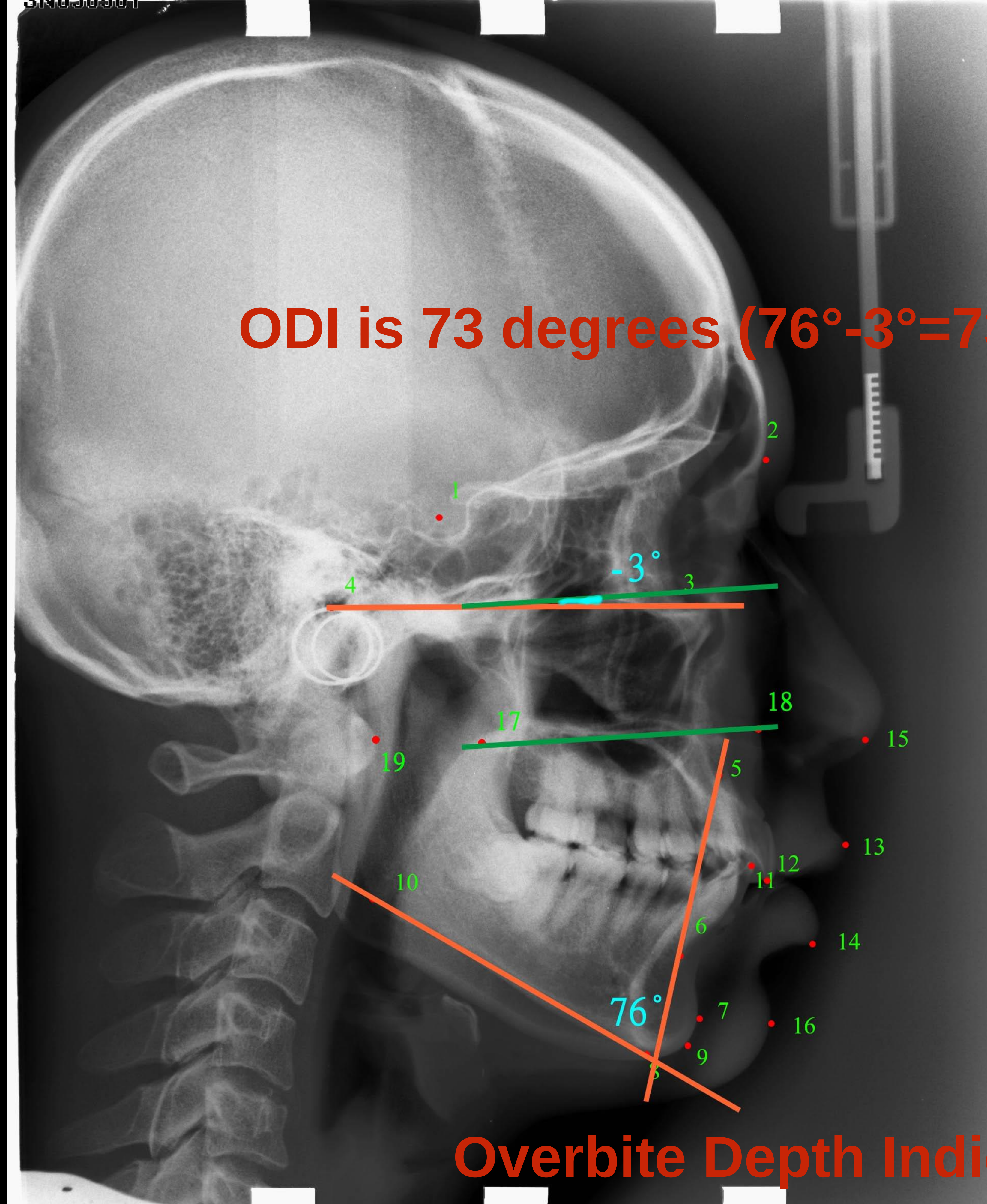

Overbite Depth Indicator (ODI)

APDI is 79° (88° + (-6°) + (-3°) = 79°)

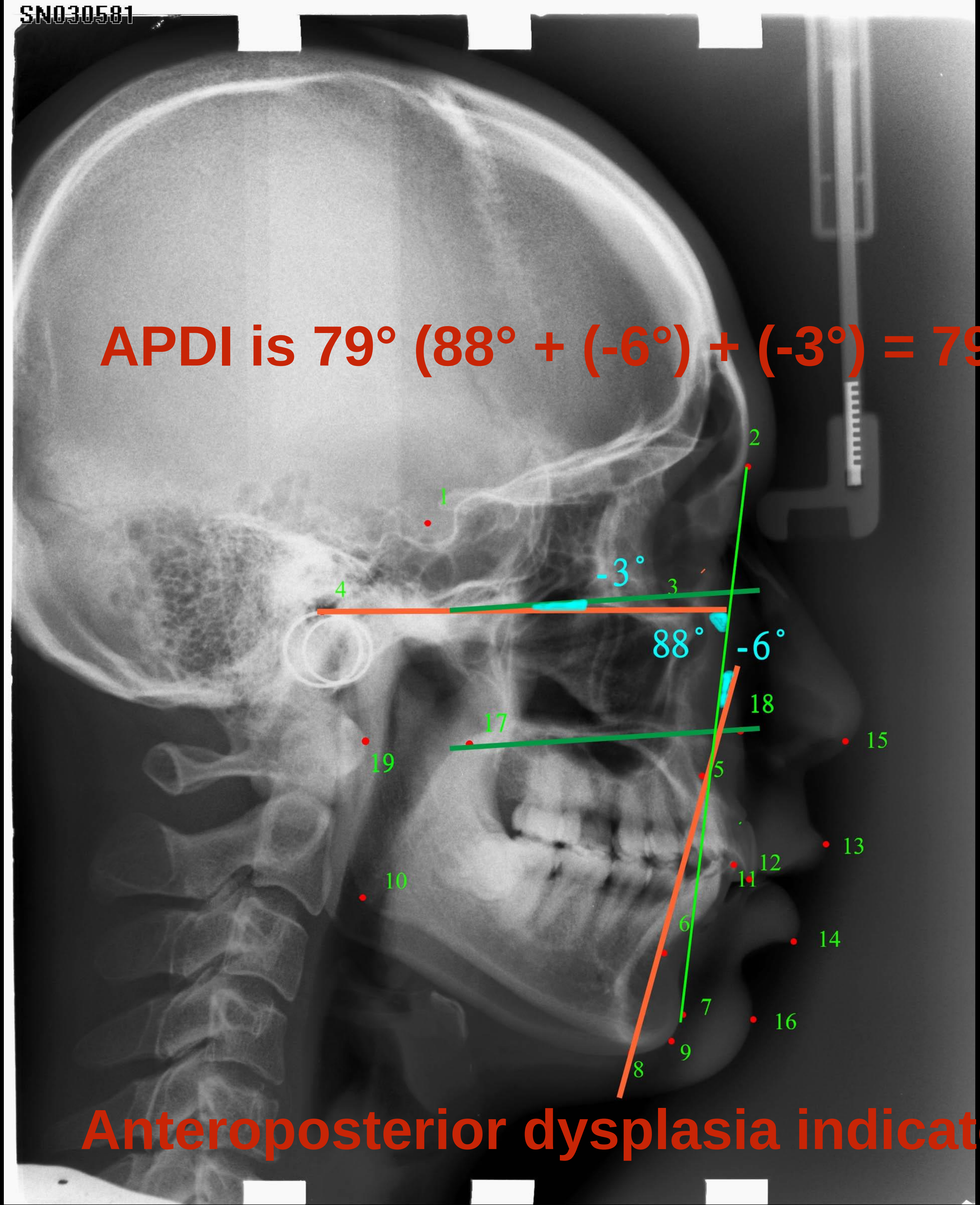

Anteroposterior dysplasia indicator (APDI)

Currently in clinical practice

- Varying levels of orthodontic training and experience may have
  - an impact on inter-observer variations,
  - time-constraints
  - other commitments may have an impact on intra-observer consistency

www.nature.com/scientificreports

SCIENTIFIC REPORTS

OPEN

Fully Automatic System for Accurate Localisation and Analysis of Cephalometric Landmarks in Lateral Cephalograms

Received: 03 May 2016
Accepted: 24 August 2016
Published: 20 September 2016

Claudia Lindner[1], Ching-Wei Wang[2,3], Cheng-Ta Huang[2,3,4], Chung-Hsing Li[5,6], Sheng-Wei Chang[5,6] & Tim F. Cootes[1]

Lindner C., Wang C*, **Huang C.**, Li C., Chang S., Cootes T. Fully Automatic System for Accurate Localisation and Analysis of Cephalometric Landmarks in Lateral Cephalograms,

Nature Scientific Reports (SCI, JCR 2015 (7/63) in MULTIDISCIPLINARY SCIENCES, IF=5.228)

Fully Automatic Landmark Annotation System

- The FALA system follows a machine learning approach where Random Forest regression-voting is used both to detect the position, scale and orientation of the skull and then,
- in the Constrained Local Model framework (RFRV-CLM), to locate the individual landmarks

Fully Automatic Landmark Annotation System

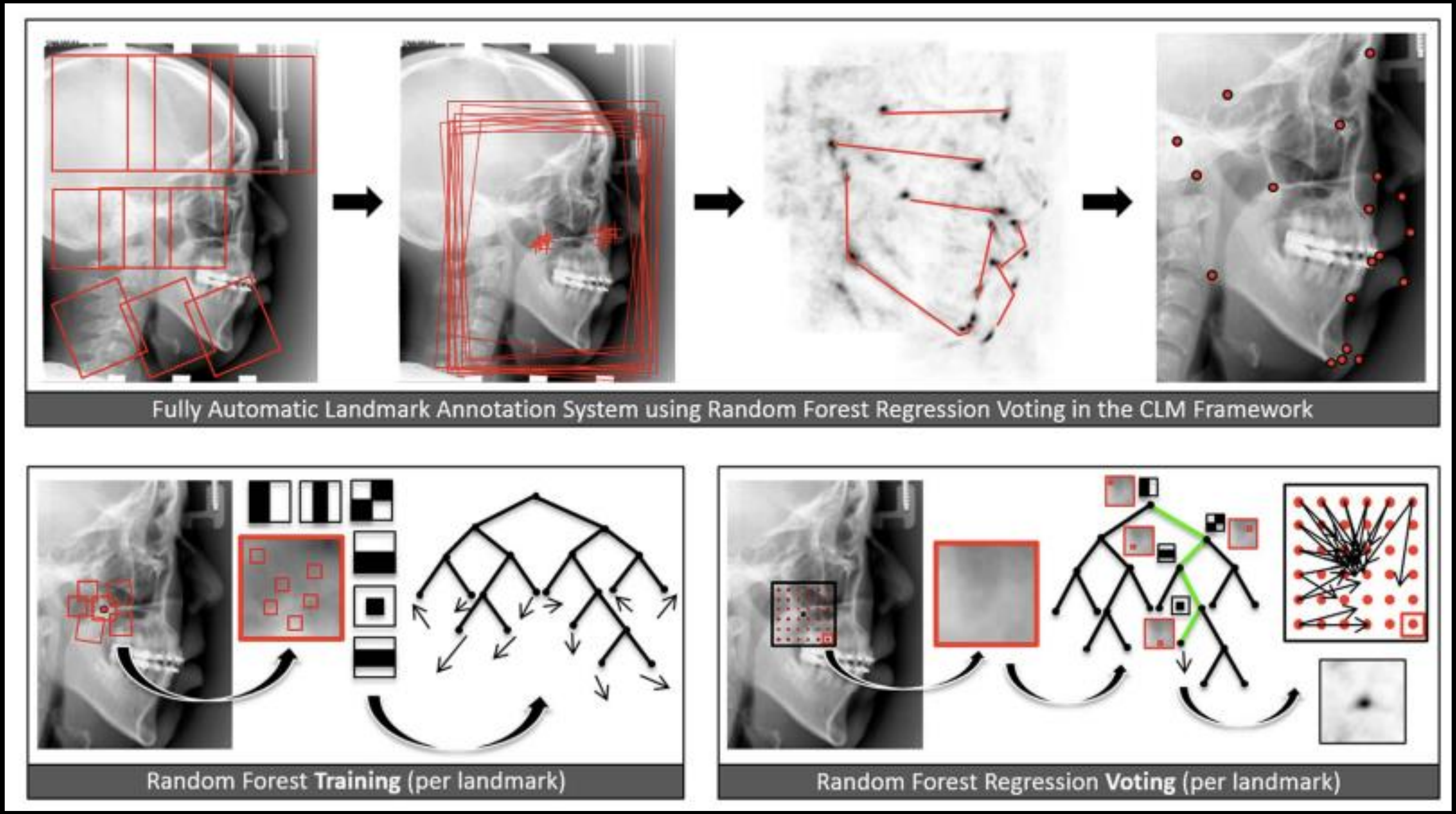

Dataset

- Lateral cephalograms were available from 400 subjects (mean age: 27.0 years; age range: 7-76 years; 235 females, 165 males).

- All cephalograms were acquired in TIFF format with a Soredex CRANEXr Excel Ceph machine (Tuusula, Finland) using Soredex SorCom software (3.1.5, version 2.0).

- The image resolution was 1935×2400 pixels with a pixel spacing of 0.1mm.

Dataset

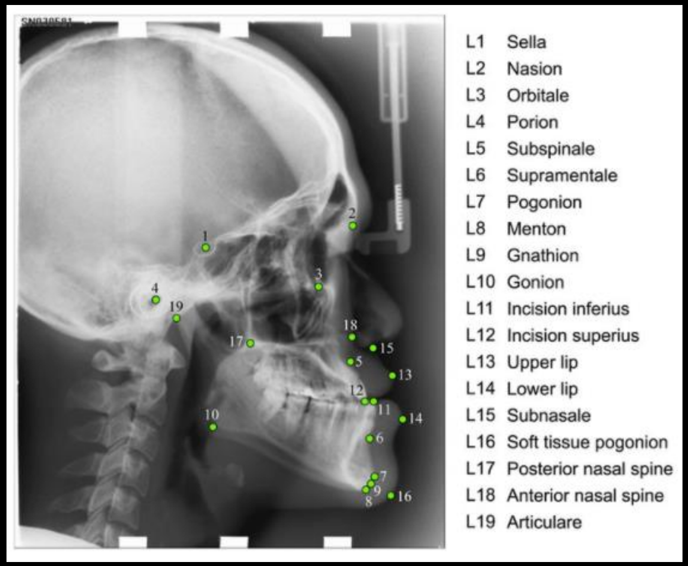

- All images were annotated ("traced") independently by two clinical orthodontists (with six years and 15 years of experience, respectively), yielding a manual annotation of 19 cephalometric landmark positions.
- For a random subset of 150 images, two sets of manual annotations per orthodontist were available.

Fully Automatic Landmark Annotation System

Landmark	PEL ± SE (mm)	SDR (%)			
		2.0 mm	2.5 mm	3.0 mm	4.0 mm
Sella (L1)	0.80 ± 0.05	96.75	98.50	98.75	99.25
Nasion (L2)	1.06 ± 0.06	85.00	90.00	91.25	96.50
Orbitale (L3)	1.24 ± 0.06	78.75	84.75	89.50	95.50
Porion (L4)	1.64 ± 0.10	79.25	83.50	86.50	89.75
Subspinale (L5)	1.44 ± 0.05	75.50	85.25	91.75	95.75
Supramentale (L6)	1.26 ± 0.05	83.00	89.50	94.50	98.75
Pogonion (L7)	1.00 ± 0.03	91.50	95.50	98.25	100.00
Menton (L8)	0.84 ± 0.03	94.75	97.50	98.75	99.25
Gnathion (L9)	0.80 ± 0.03	97.00	99.00	99.50	99.50
Gonion (L10)	2.69 ± 0.12	50.25	57.00	65.25	79.75
Incision inferius (L11)	0.89 ± 0.06	89.25	91.00	94.25	97.50
Incision superius (L12)	0.65 ± 0.05	92.25	93.50	95.25	98.50
Upper lip (L13)	1.22 ± 0.04	83.50	93.00	98.25	99.75
Lower lip (L14)	0.92 ± 0.04	94.25	97.75	98.75	99.75
Subnasale (L15)	1.15 ± 0.05	87.00	90.00	91.50	96.75
Soft tissue pogonion (L16)	1.23 ± 0.06	83.50	90.75	94.50	98.00
Posterior nasal spine (L17)	0.96 ± 0.05	94.00	95.50	96.75	97.75
Anterior nasal spine (L18)	1.49 ± 0.07	77.00	82.50	87.75	93.25
Articulare (L19)	1.43 ± 0.08	76.75	83.75	88.75	94.50
Average	1.20 ± 0.06	84.70	89.38	92.62	96.30

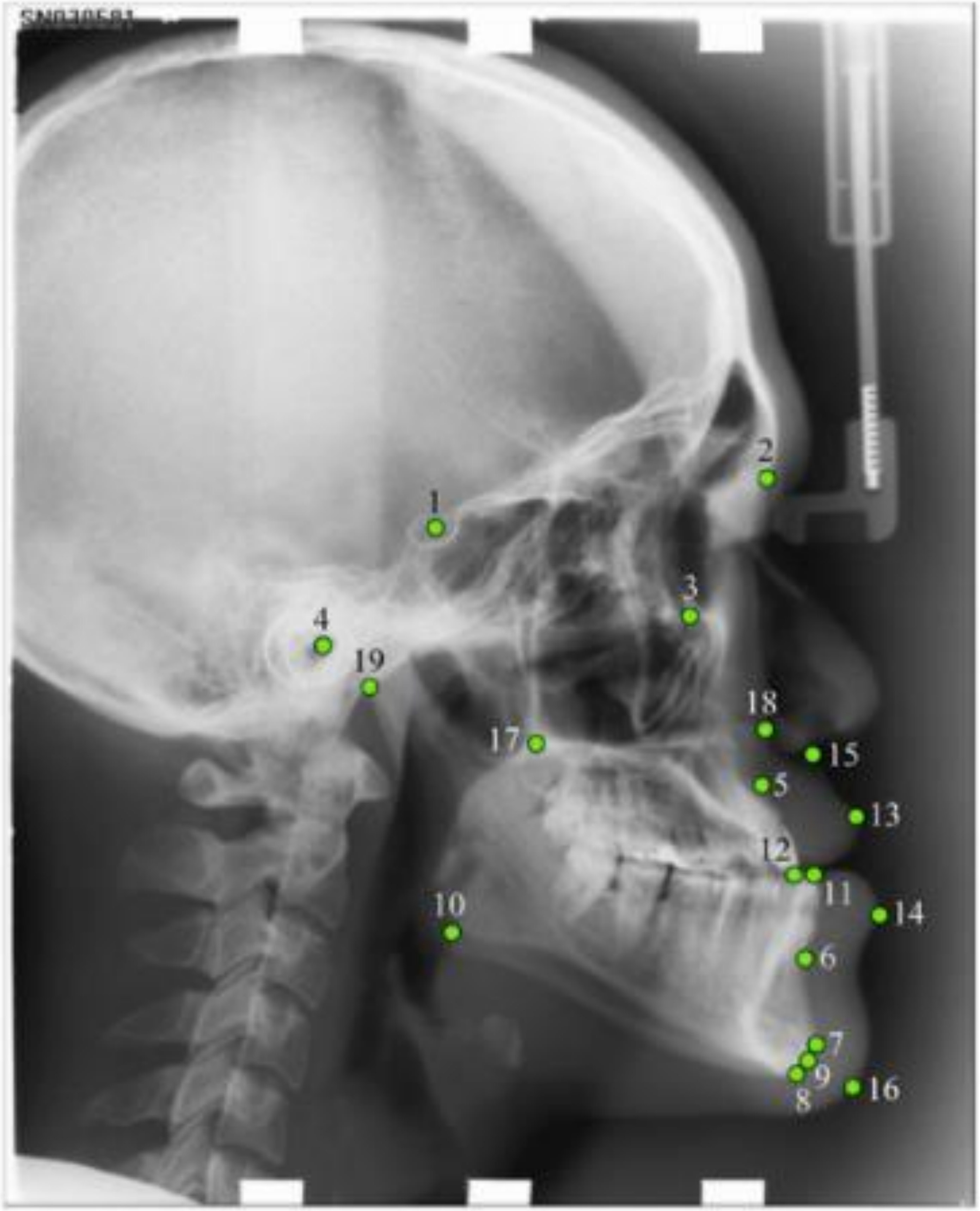

- L1 Sella
- L2 Nasion
- L3 Orbitale
- L4 Porion
- L5 Subspinale
- L6 Supramentale
- L7 Pogonion
- L8 Menton
- L9 Gnathion
- L10 Gonion
- L11 Incision inferius
- L12 Incision superius
- L13 Upper lip
- L14 Lower lip
- L15 Subnasale
- L16 Soft tissue pogonion
- L17 Posterior nasal spine
- L18 Anterior nasal spine
- L19 Articulare

Computer-Automated Detection of Caries in Bitewing Radiography

- ISBI 2015, NewYork, USA
- http://www-o.ntust.edu.tw/~cweiwang/ISBI2015/challenge2/

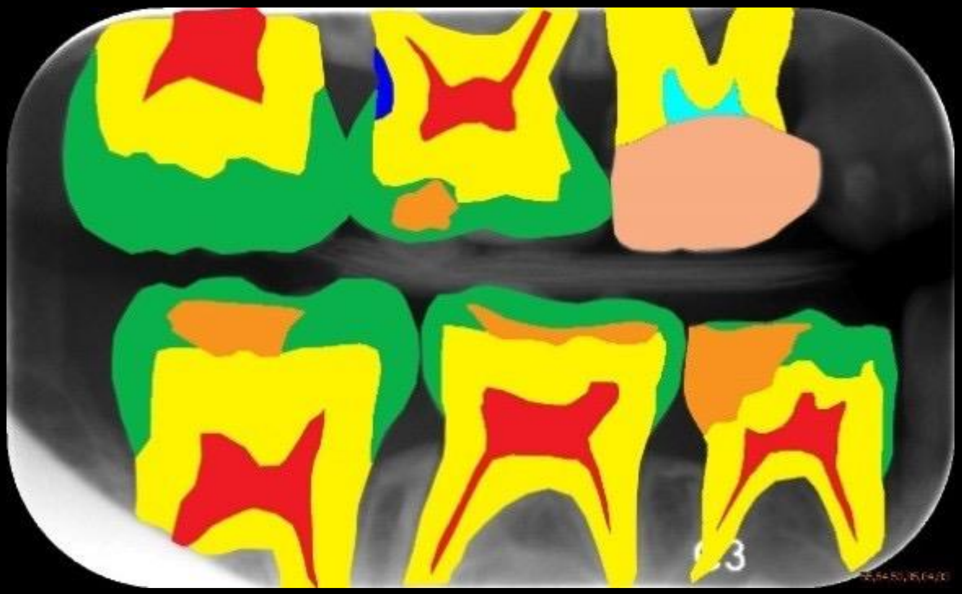

Computer-Automated Detection of Caries in Bitewing Radiography

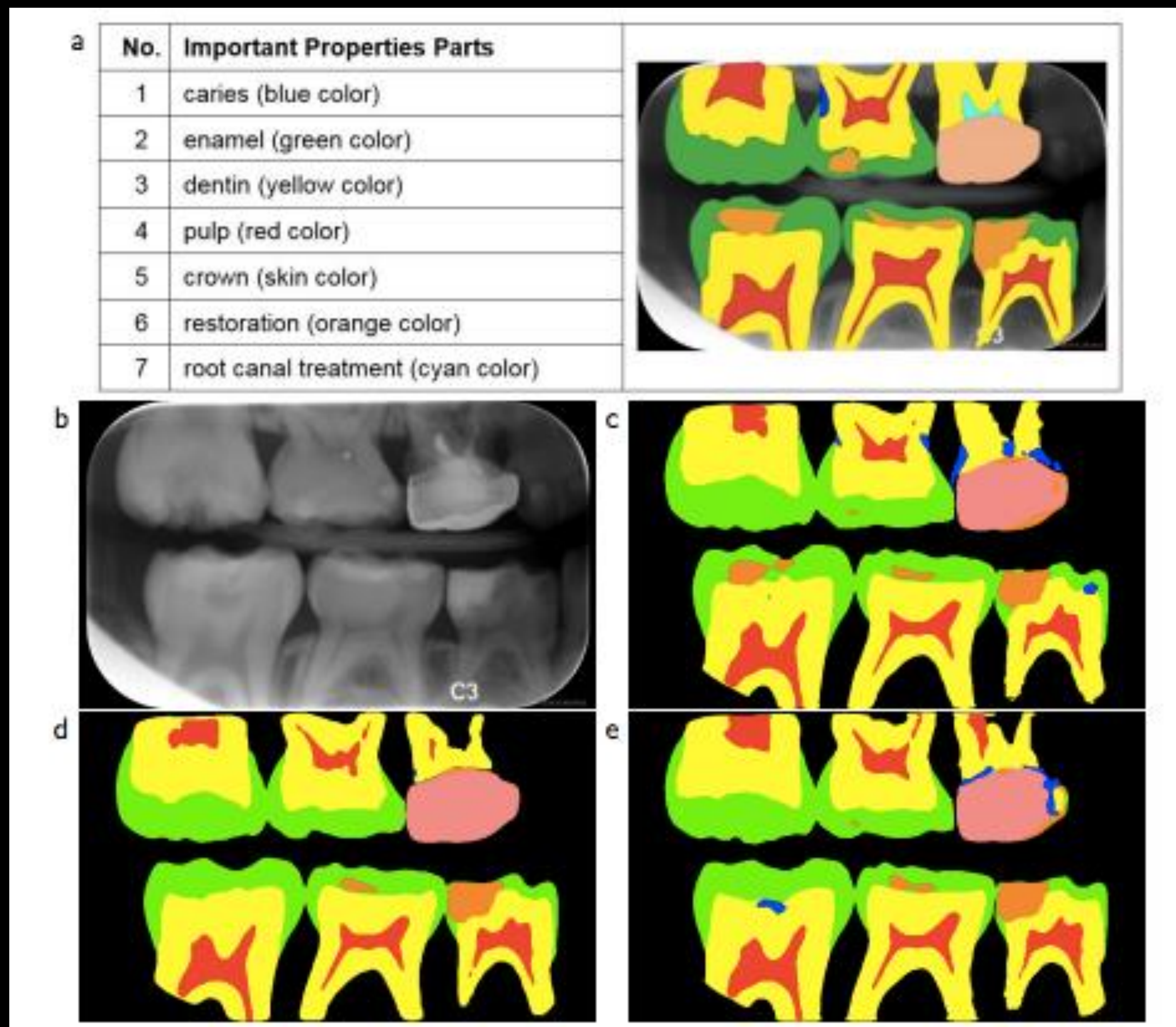

Fig. 4. Example results for sample 46. (**a**) legend and manual ground truth from the challenge web page. (**b**) input x-ray image. (**c**) result of u-net architecture "u1" (**d**) architecture "u2" (**e**) architecture "u3"

4D MRI 心臟左右心室分割

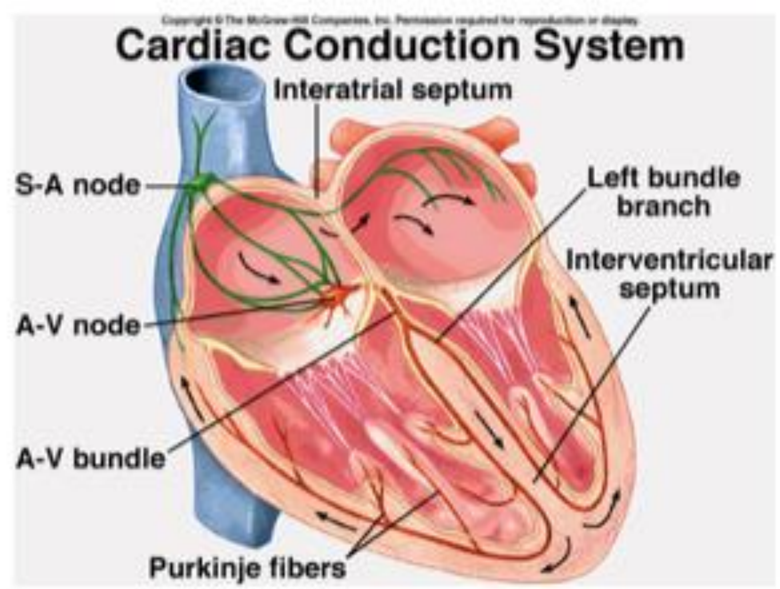

4D MRI 心臟左右心室分割

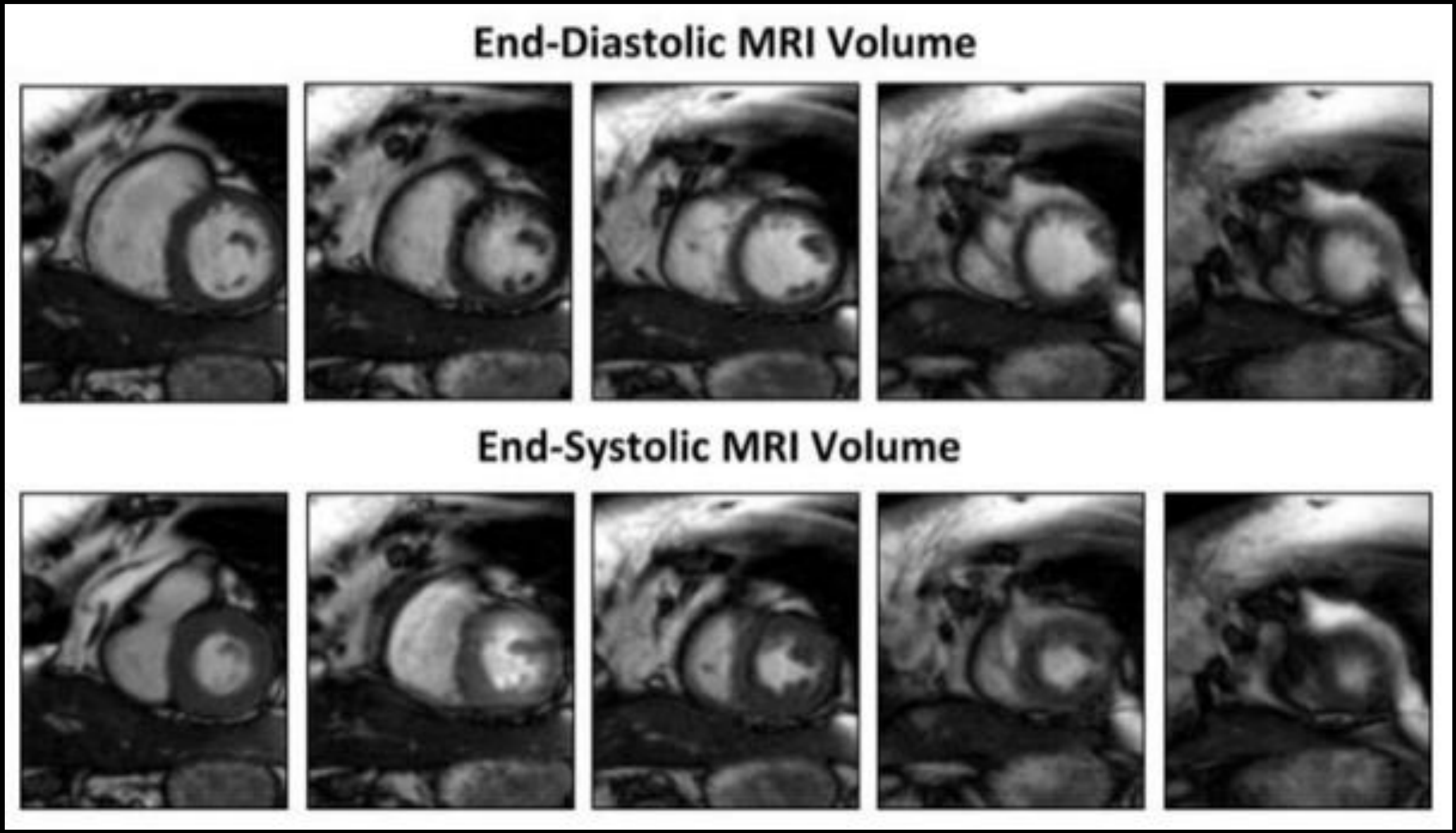

4D MRI 心臟左右心室分割

binary difference of Gaussian (DoG) filters

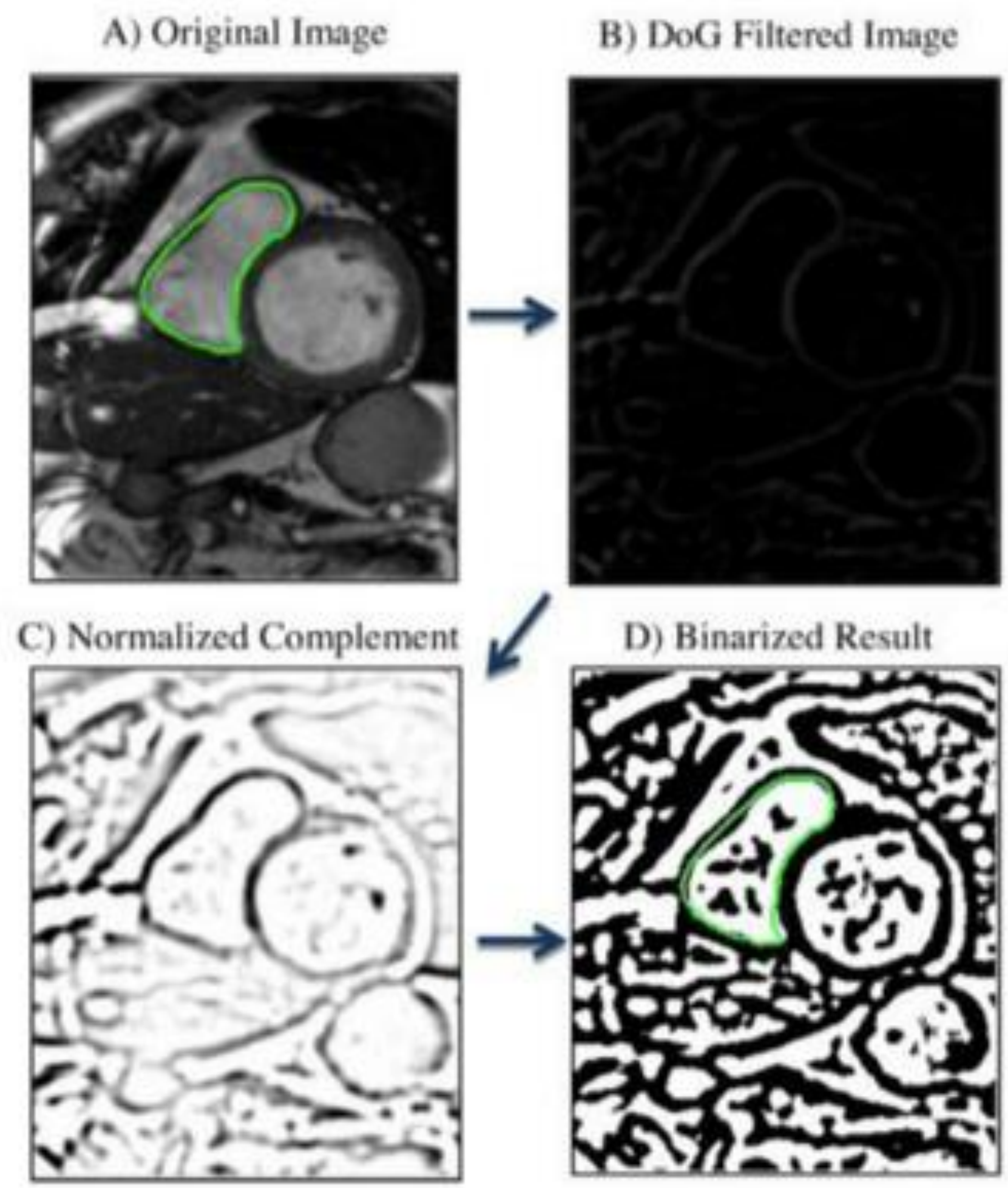

4D MRI 心臟左右心室分割

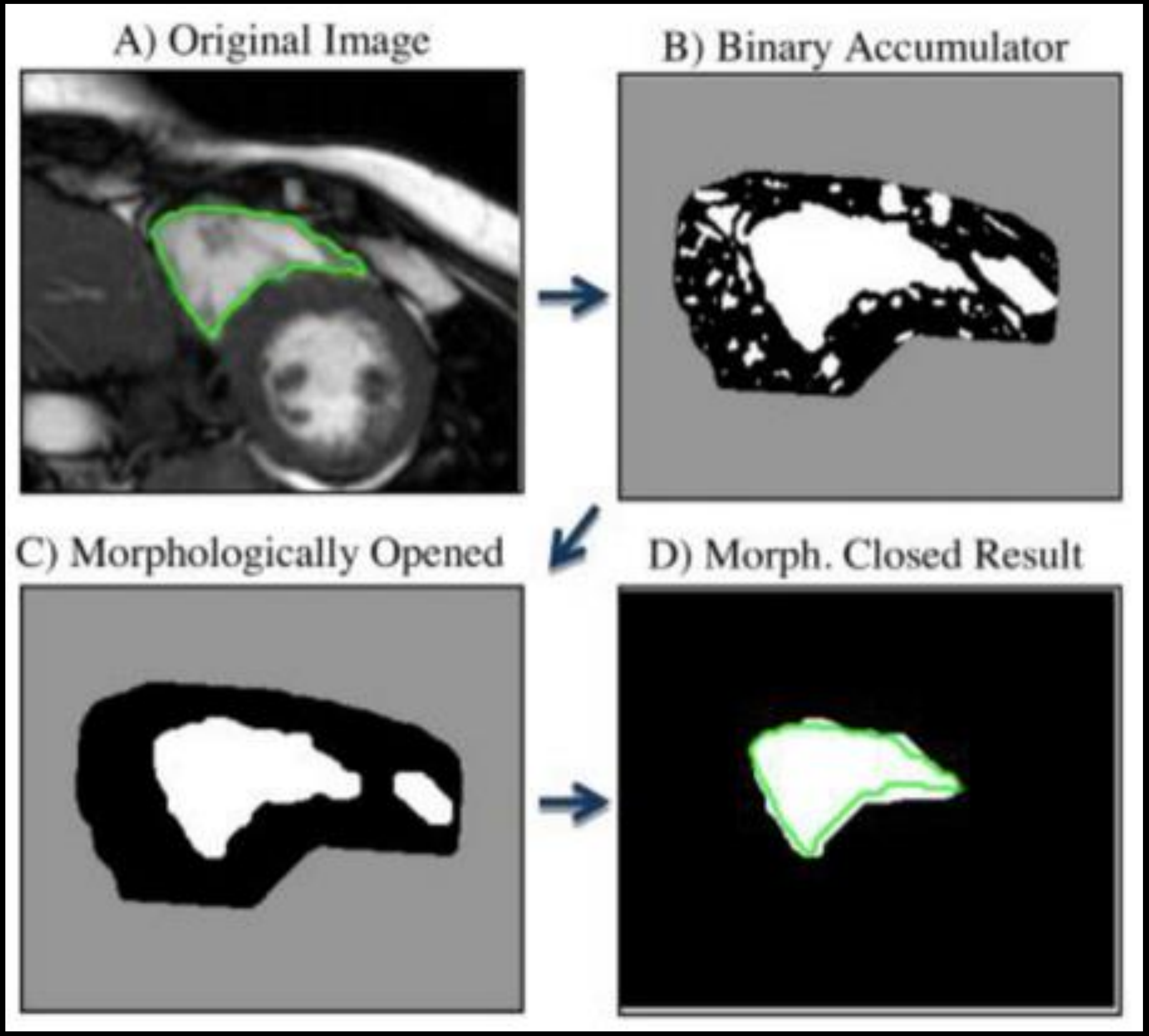

4D MRI 心臟左右心室分割

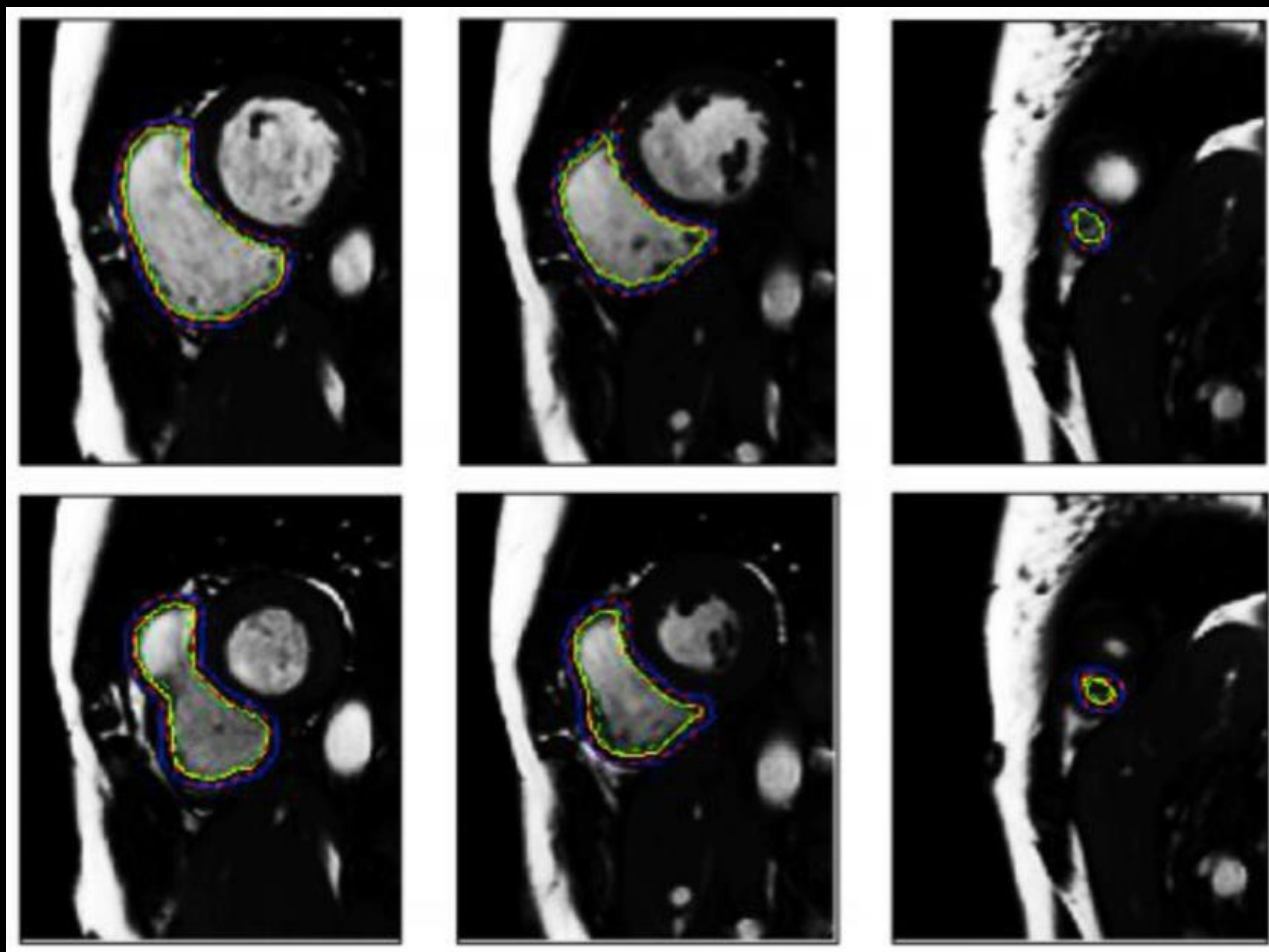

肝臟自動化分割技術

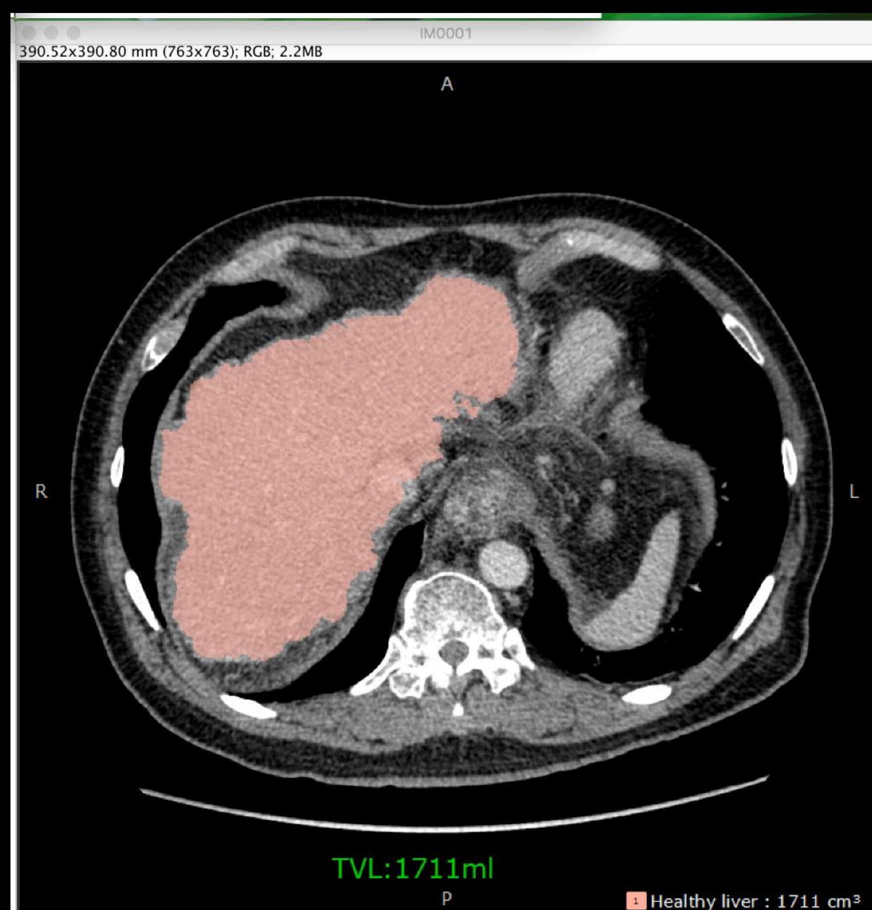
IM0001
390.52x390.80 mm (763x763); RGB; 2.2MB
A
R
L
TVL:1711ml
P
Healthy liver : 1711 cm³

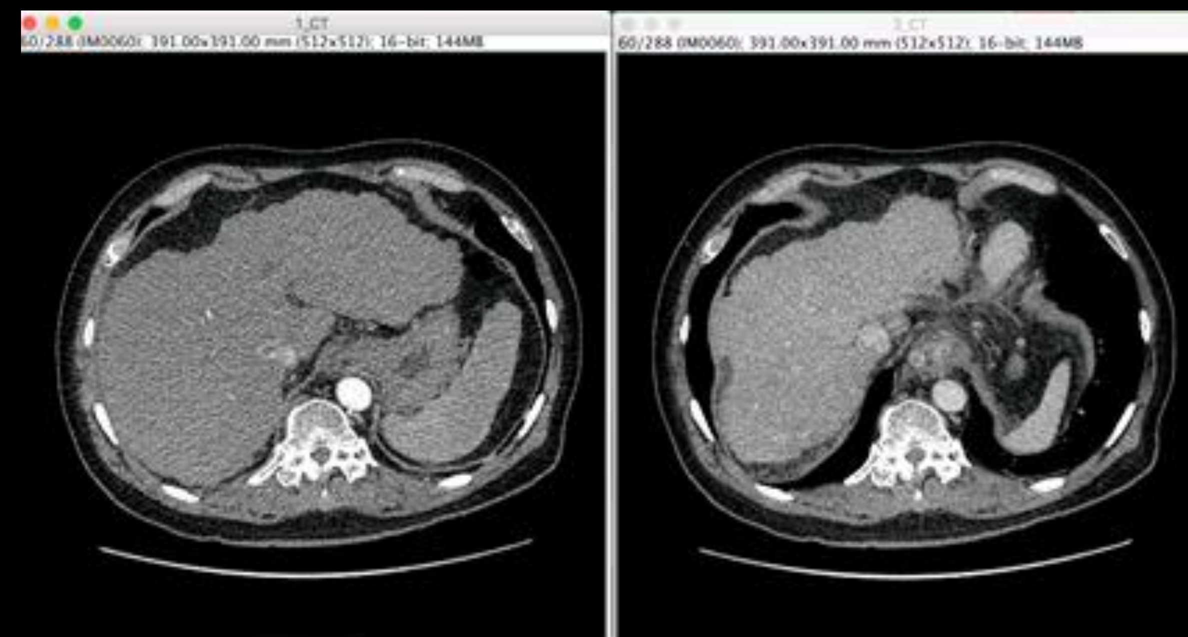

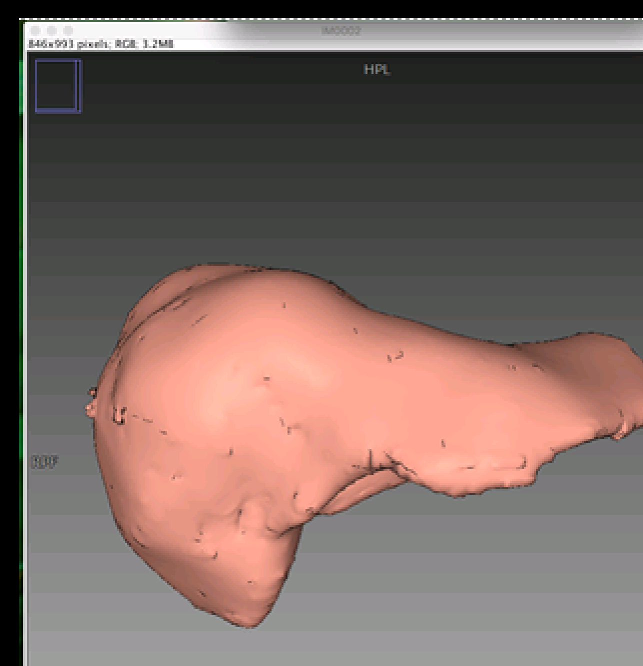
HPL

肝臟自動化分割技術

- 肝癌的外科治療是肝癌病人獲得長期生存最重要的手段，主要包括
  - 肝切除術
  - 肝移植術

肝臟自動化分割技術

- 目前臨床針對肝切除術的基本原則大致可分成
- （1）徹底性：完整切除腫瘤，使切緣無殘留腫瘤。
- （2）安全性：保留有足夠功能肝組織（具有良好血供以及良好的血液和膽汁迴流）以術後肝功能代償，降低手術死亡率及手術併發症。

影像前處理

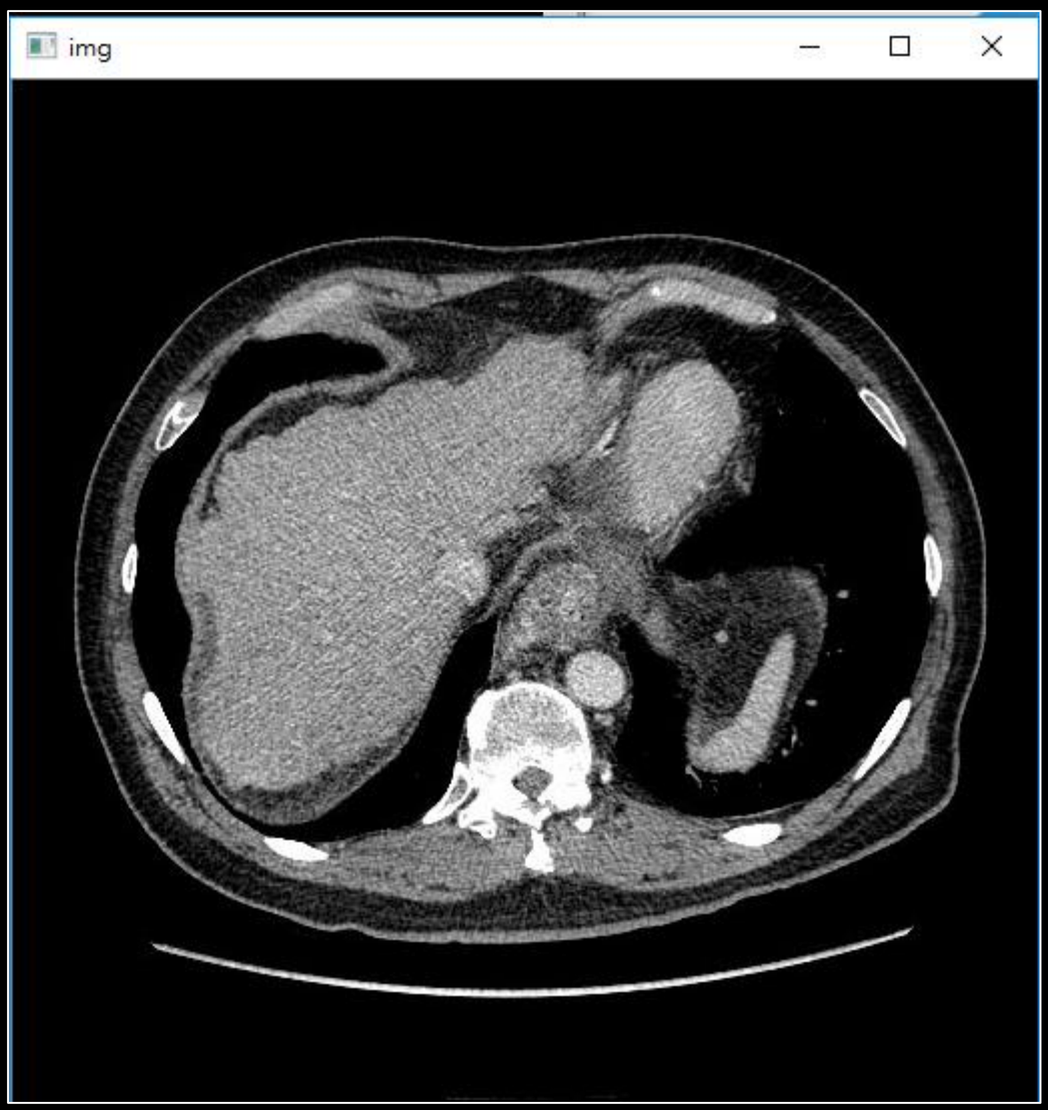

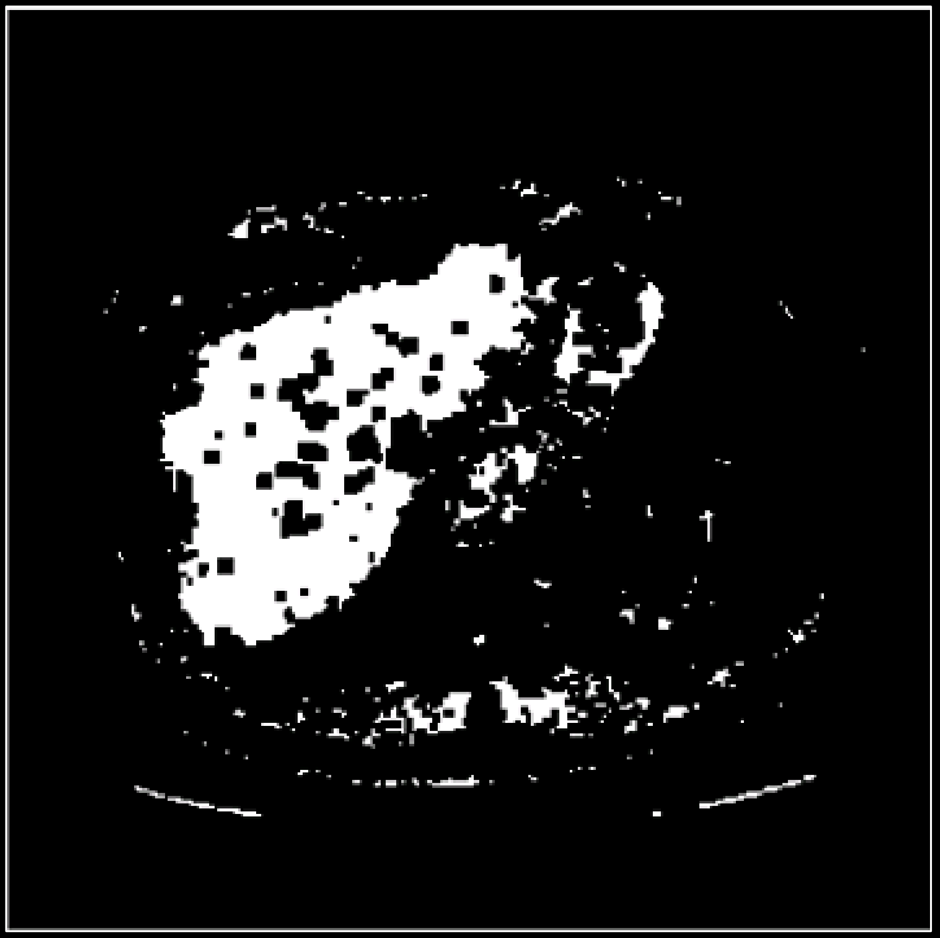

影像物件化

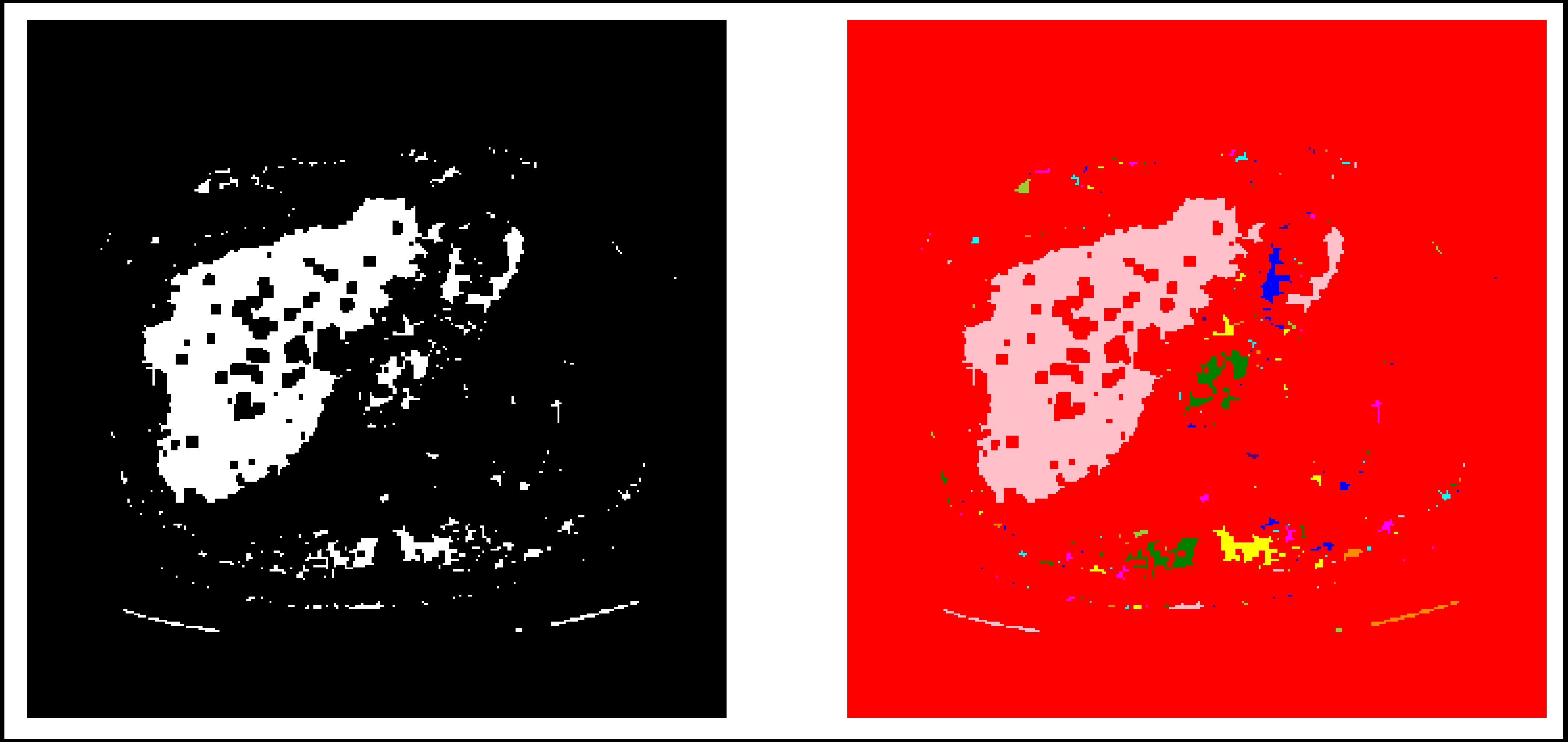

去小島

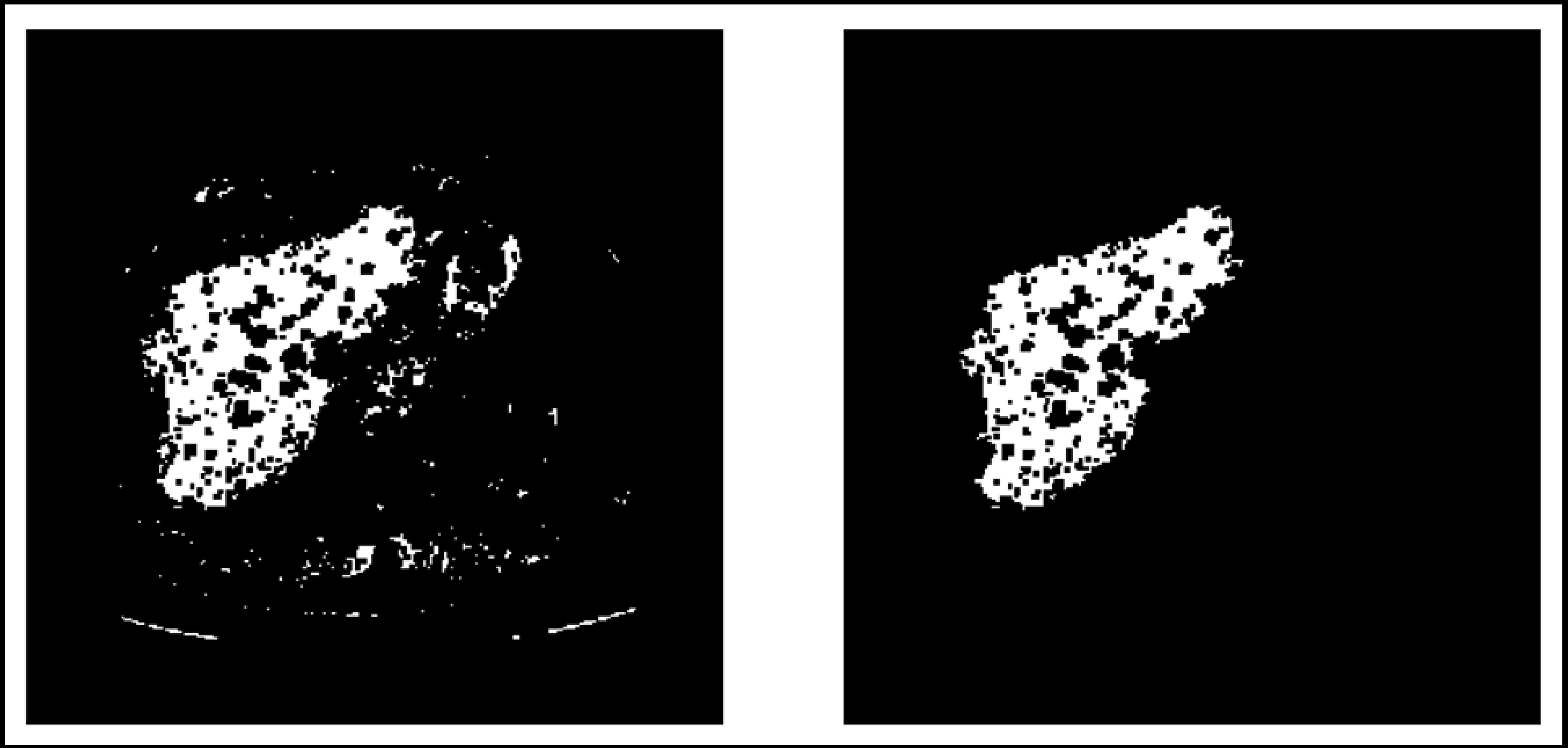

進行閉合

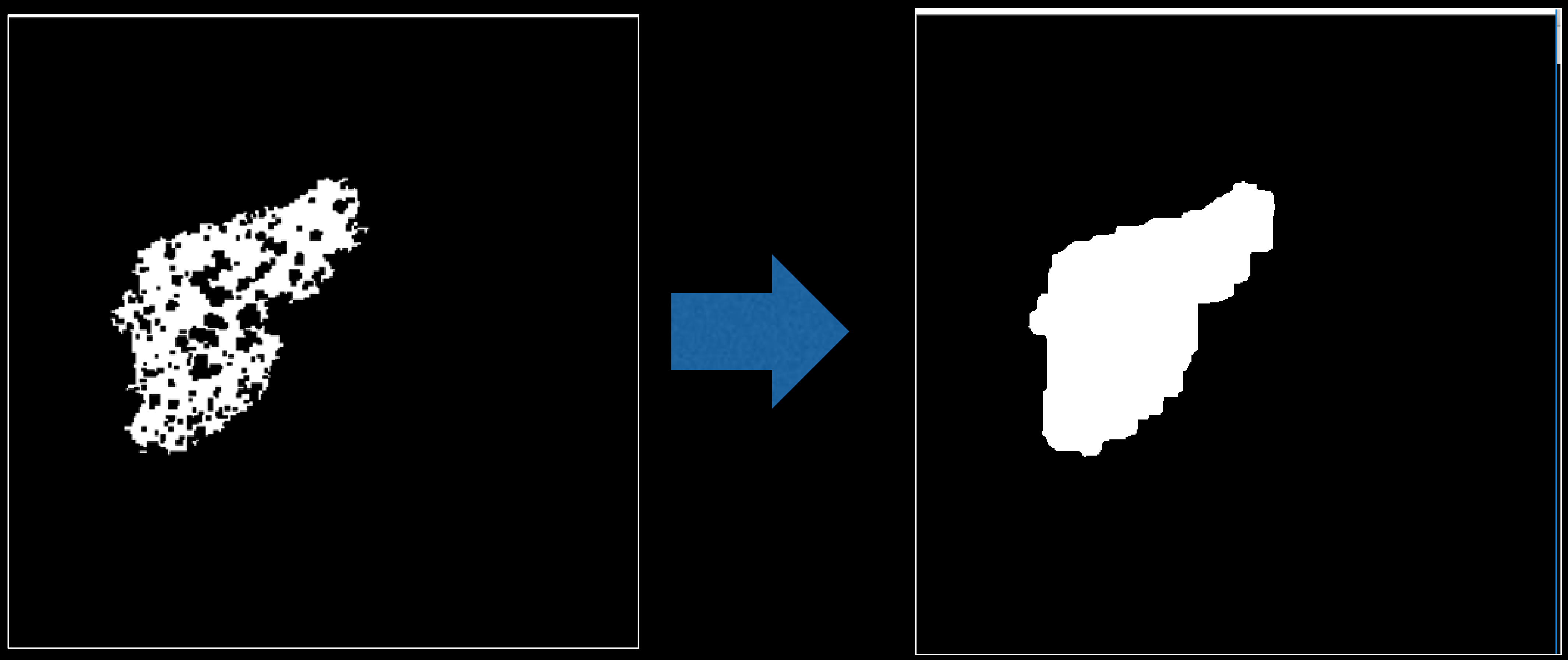

初步成果

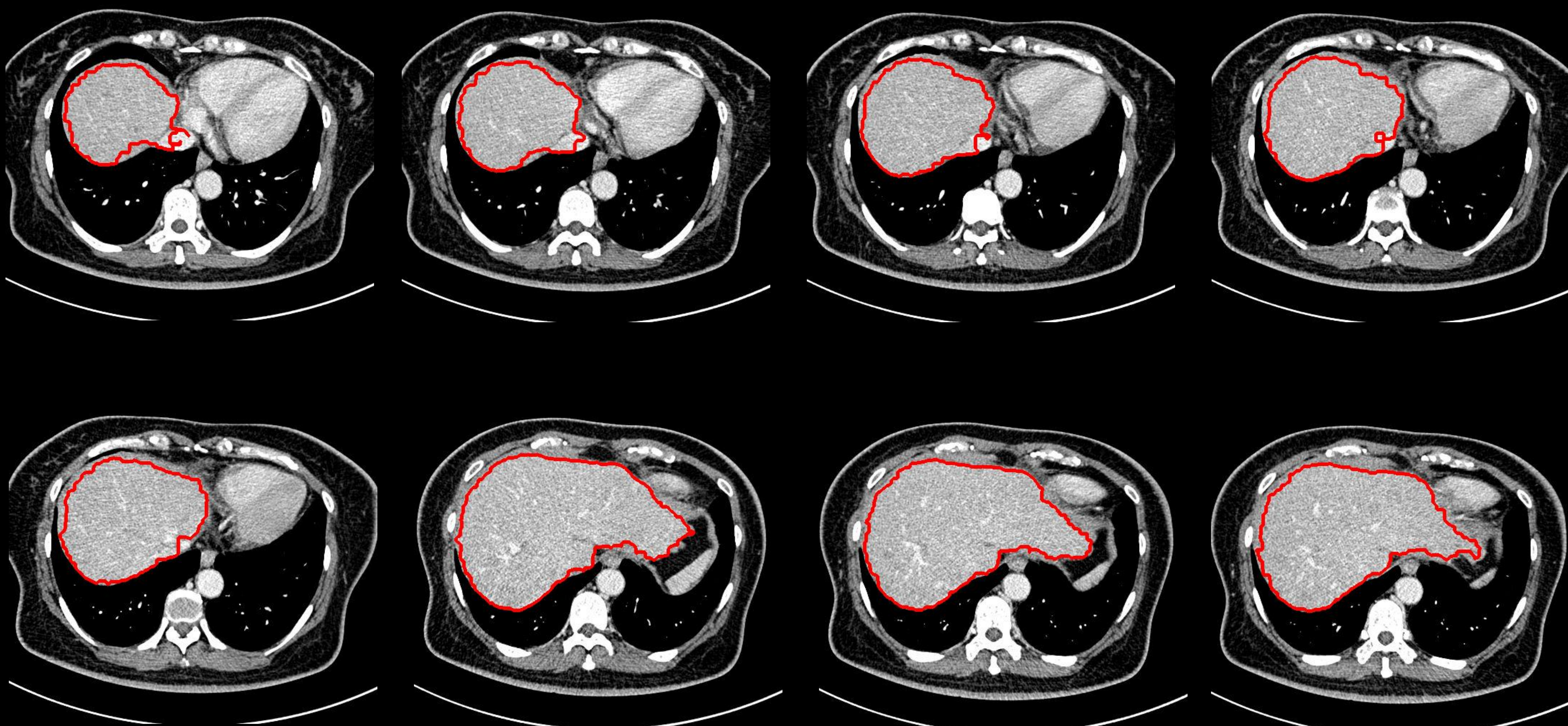

初步成果

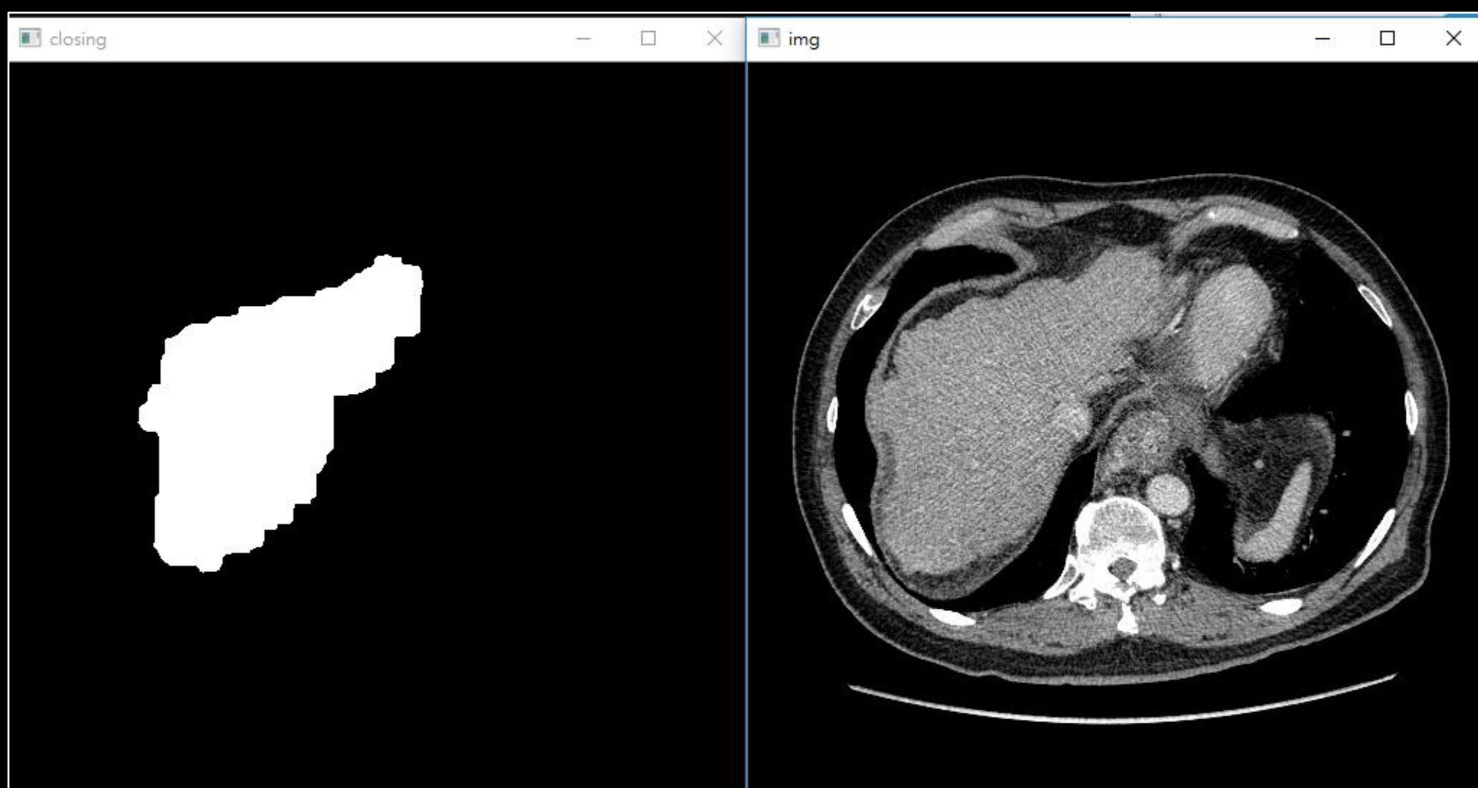

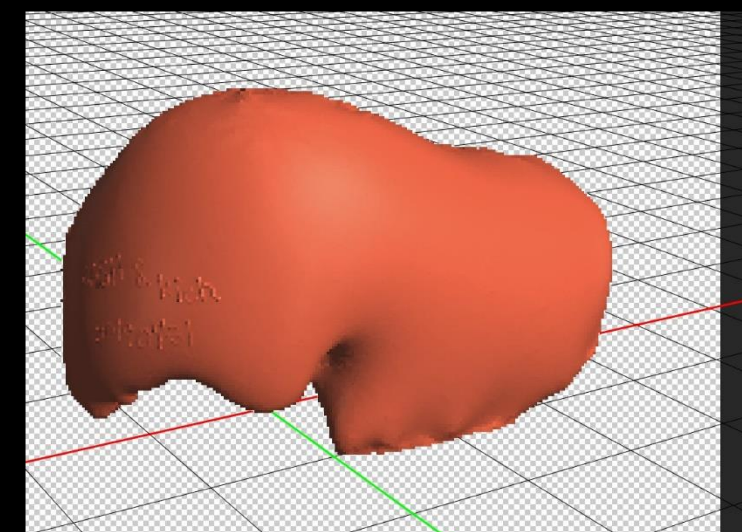

資訊科技 x 醫療影像

Mixed Reality is ready

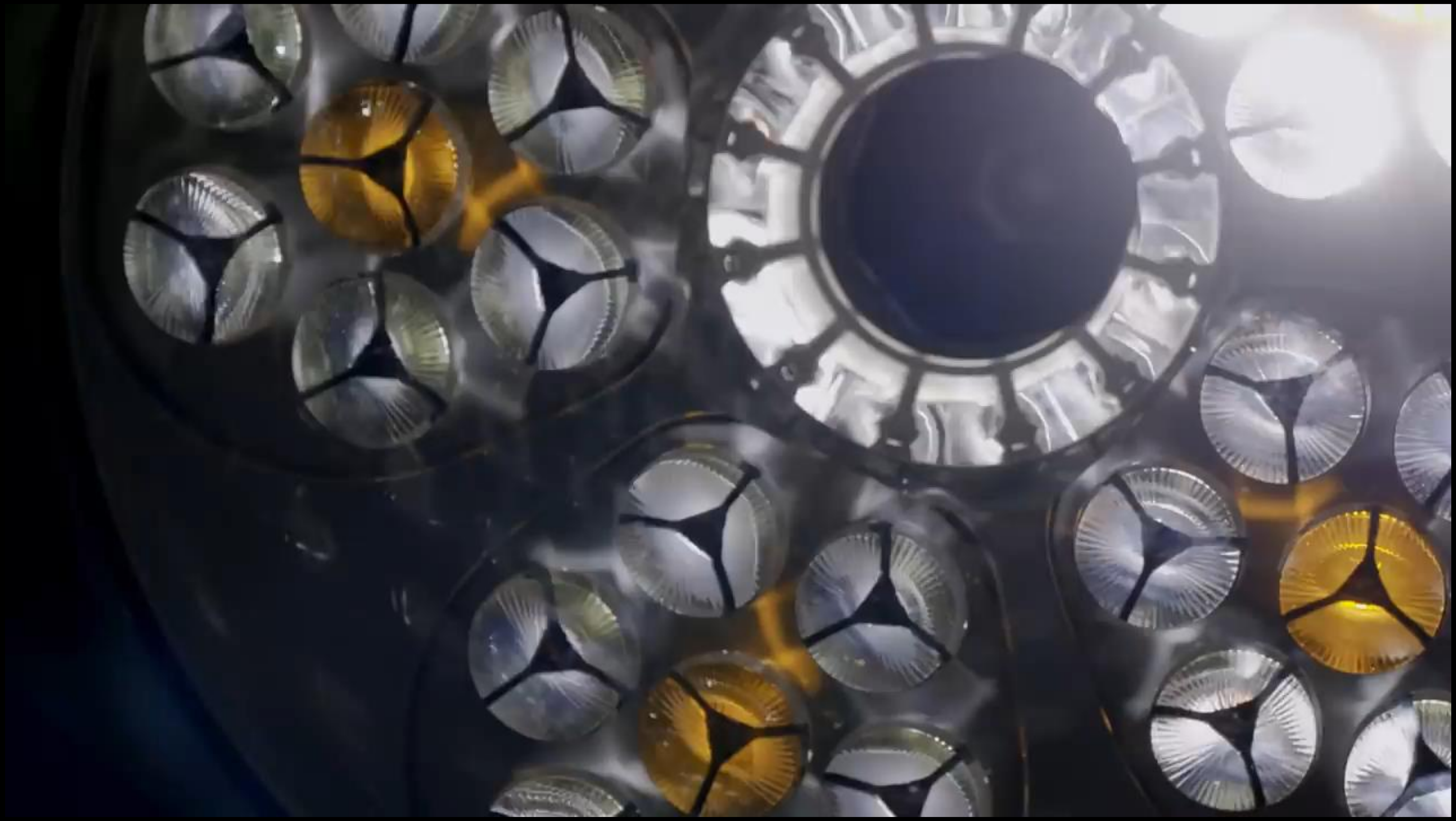

Microsoft HoloLens 2 Partner Spotlight
with Philips

Microsoft HoloLens

1. Dentist makes detailed diagnosis through micro camera

2. Shared Decision Making (SDM) in clinical practice

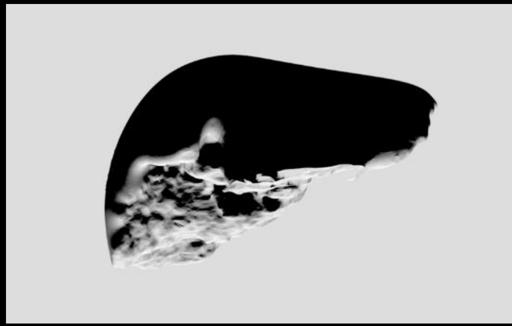

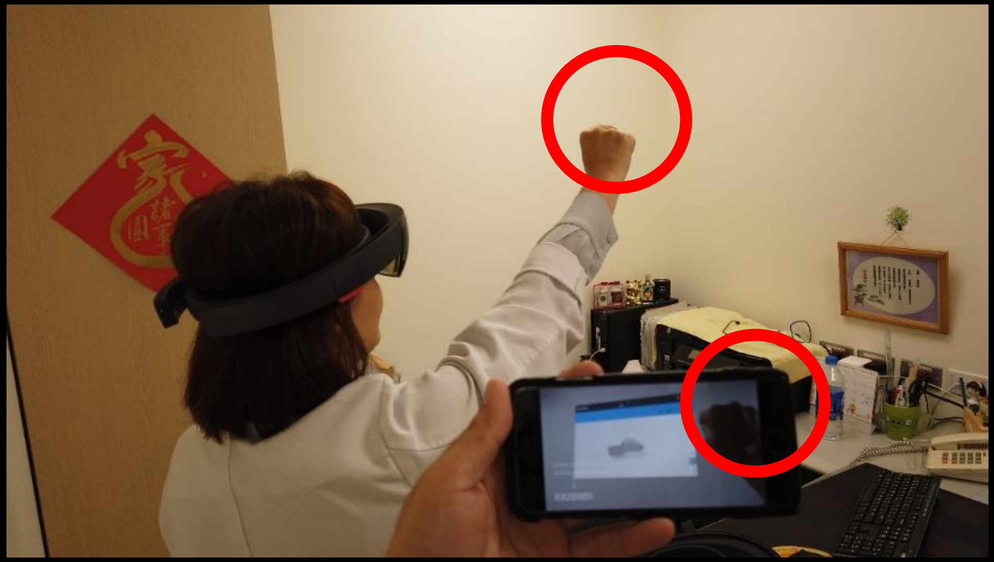

資訊科技 x 醫療影像 (肝臟)

資訊科技 x 醫療影像 (心臟 骨盆腔)

HoloLens Demo

影像上的資訊安全 -
版權保護

資訊隱藏

- **Information Hiding**
  - Many forms: in text, watermark, audio, image, MP3, video
    - Much more different than Cryptography (codes and ciphers)
    - Steganography is the art and science of communicating in a way which hides the existence of the communication.
    - Watermarking imprints a distinctive mark so that one can use it for identification purposes.

The “Magic” Rhombus

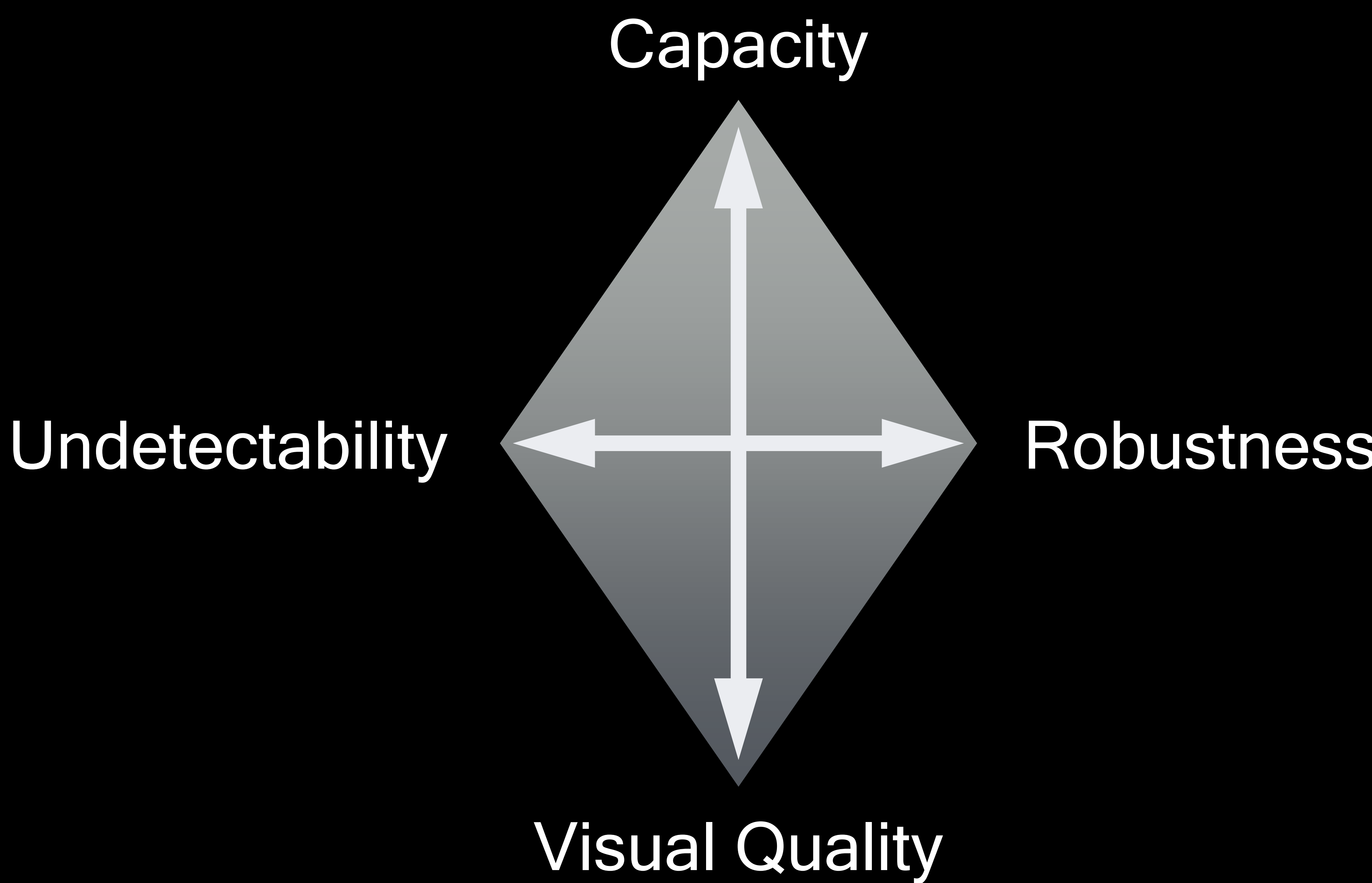

Steganography for Images

- **Three domains**
  - **Spatial domain**
    - Least Significant Bit, LSB
    - Histogram statistics
    - Pixel Value Difference
    - …
  - **Frequency domain**
    - Discrete Wavelet Transform, DWT
    - Discrete Cosine Transform, DWT
    - …
  - **Compression domain**
    - Vector Quantization, VQ
    - Side-Match VQ, SMVQ
    - Search order coding, SOC
    - …

Vector Quantization

- In 1980, Linde, Buzo and Gray (**LBG**) proposed a VQ design algorithm based on a training sequence.
  - **High compression rate**
  - **Fast decoding efficiency**

Vector Quantization

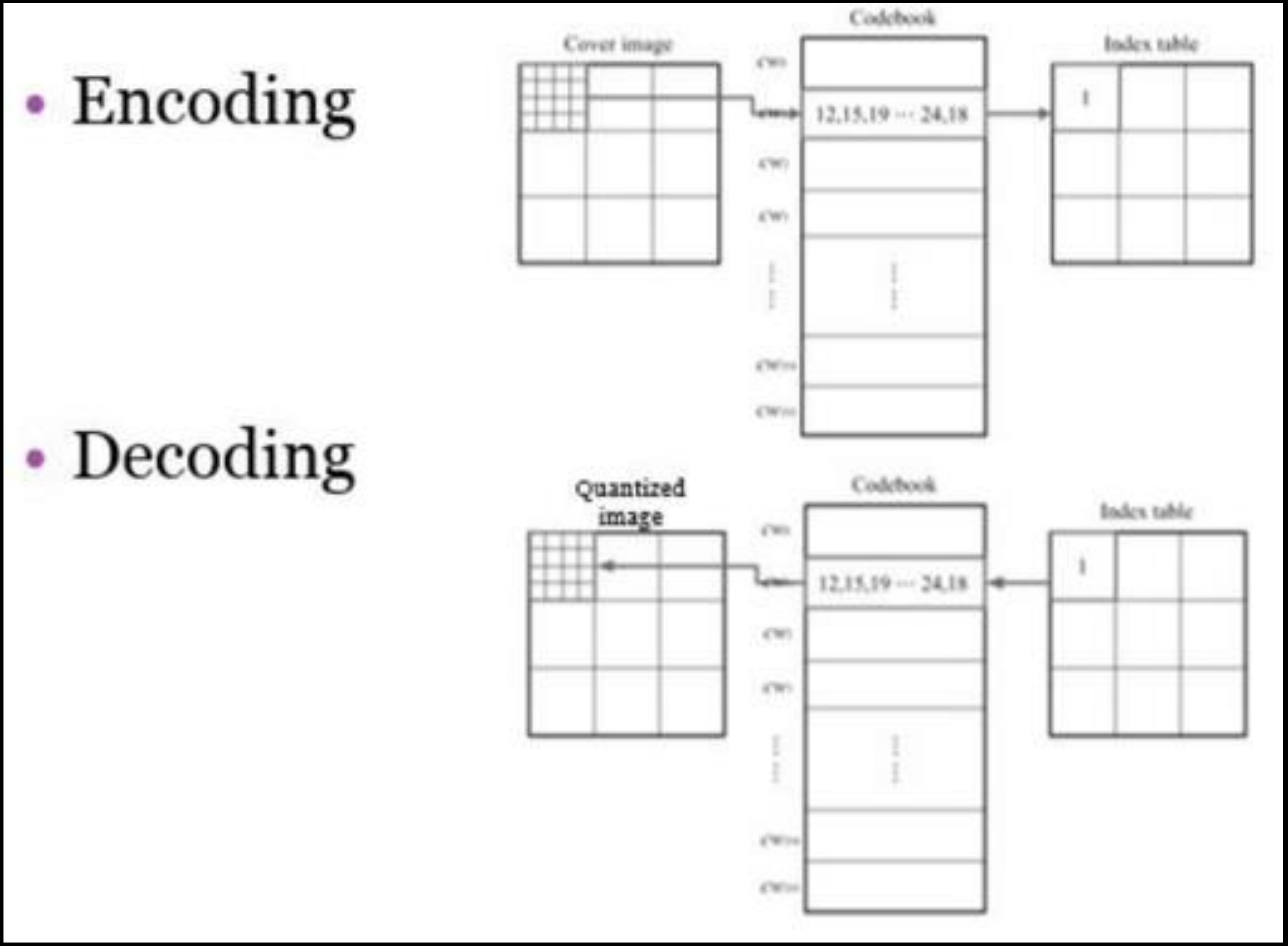

Vector Quantization

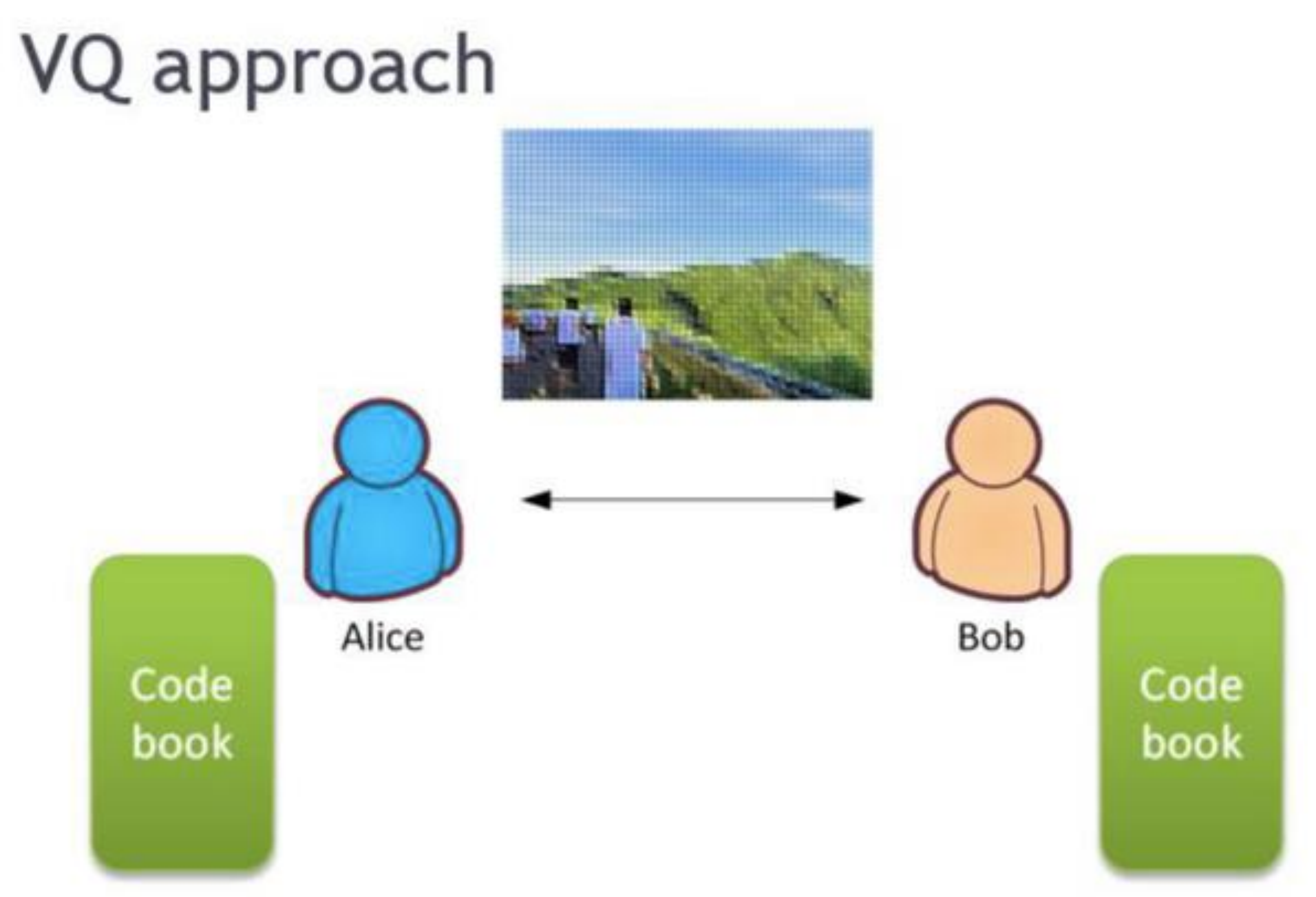

Vector Quantization

- But, if the codebooks are different

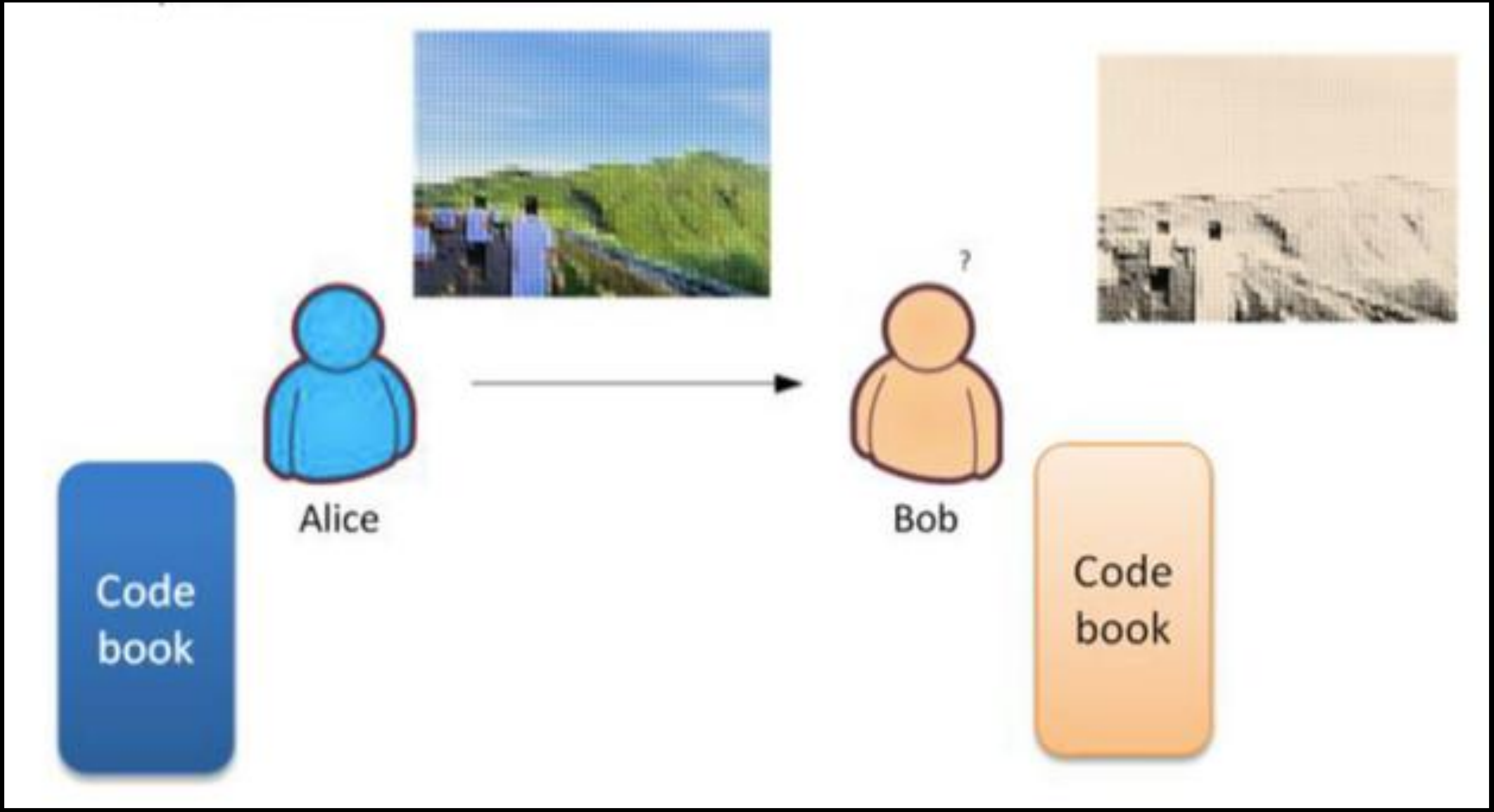

Publication

1. **CT Huang**, CH Yang, WJ Wang, SR Tsui, SJ Wang, "Raw reversibility of information hiding on the basis of VQ systems," *The Journal of Supercomputing*, 1-30, 2017 (SCI, IF: 1.088).
2. WJ Wang, **CT Huang**, SR Tsuei, SJ Wang, "A greedy steganographic SMVQ approach of greedy-USBIRDS using secret bits for image-block repairing based on differences," *Multimedia Tools and Applications* 75 (22), 14895-14916, 2016 (SCI, IF: 1.331).
3. **CT Huang**, MY Tsai, LC Lin, WJ Wang, SJ Wang, "VQ-based data hiding in IoT networks using two-level encoding with adaptive pixel replacements," *The Journal of Supercomputing*, 1-20, 2016 (SCI, IF: 1.088).
4. YT Chang, **CT Huang**, CL Huang, SJ Wang, "Data hiding of high compression ratio in VQ indices with neighboring correlations," *Multimedia Tools and Applications* 74 (5), 1645-1666, 2015 (SCI, IF: 1.331).
5. WJ Wang, **CT Huang**, SJ Wang, "VQ-encoded images in reversible data hiding of high bit-compression-ratio," *The Imaging Science Journal* 63 (1), 24-33, 2015 (SCI, IF: 0.454).

WJ Wang, **CT Huang**, SR Tsuei, SJ Wang, "A greedy steganographic SMVQ approach of greedy-USBIRDS using secret bits for image-block repairing based on differences," Multimedia Tools and Applications 75 (22), 14895-14916, 2016 (SCI, IF: 1.331).

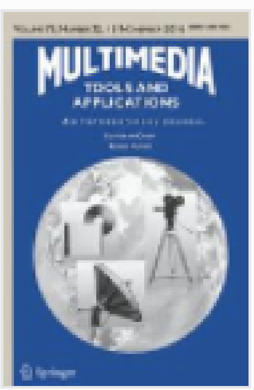

Multimedia Tools and Applications
November 2016, Volume 75, Issue 22, pp 14895–14916

A greedy steganographic SMVQ approach of greedy-USBIRDS using secret bits for image-block repairing based on differences

Authors | Authors and affiliations

Wei-Jen Wang, Cheng-Ta Huang, Shiau-Rung Tsuei, Shiuh-Jeng WANG

Article

First Online: 09 July 2015

DOI: 10.1007/s11042-015-2761-8

Cite this article as:
Wang, WJ., Huang, CT., Tsuei, SR. et al. Multimed Tools Appl (2016) 75: 14895. doi:10.1007/s11042-015-2761-8

The embedding flowchart of the proposed algorithm

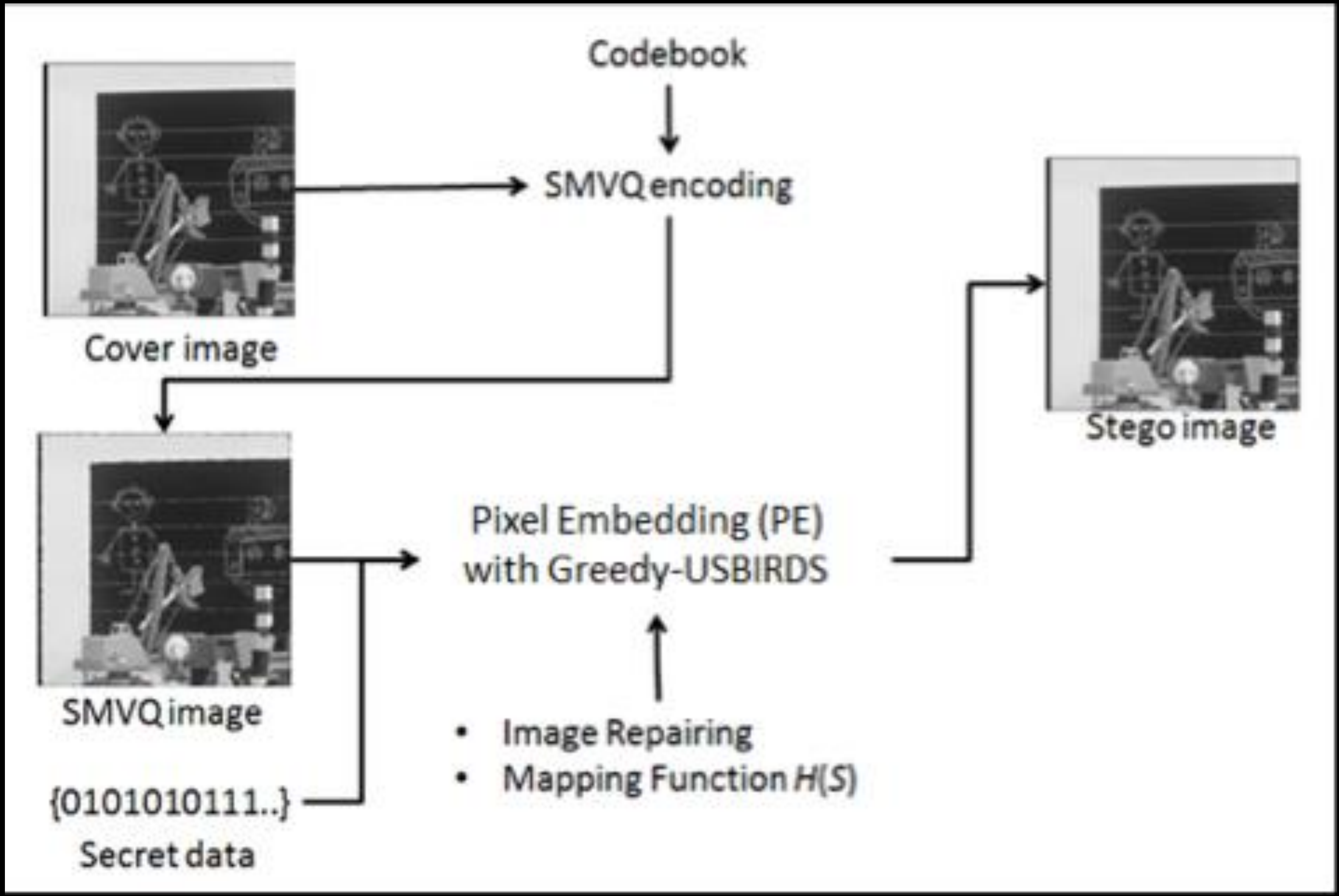

The extracting flowchart of the proposed algorithm

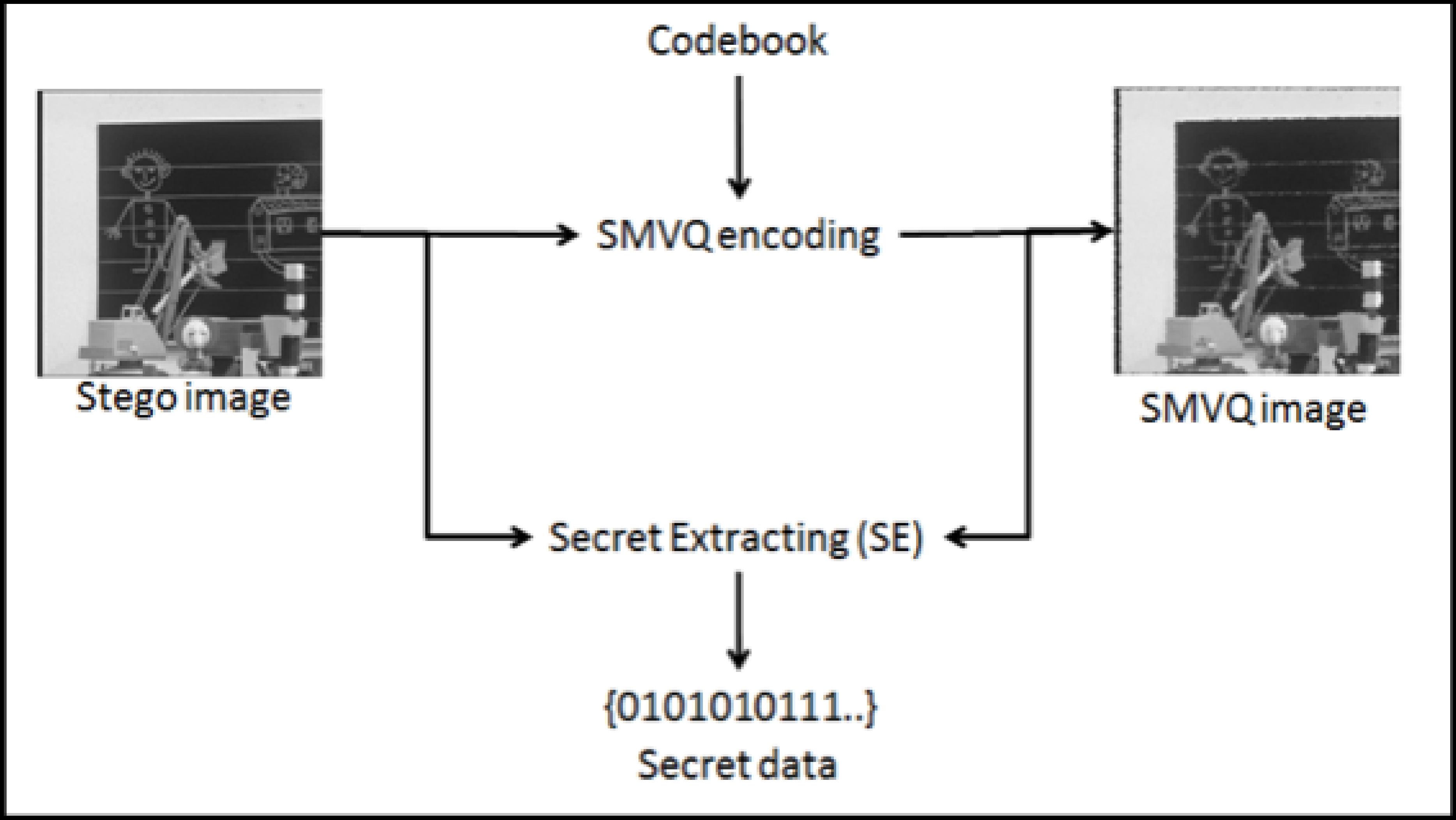

Concept of the proposed Greedy-USBIRDS method

- The proposed method uses two major techniques based on SMVQ:
  - 1. Image repairing technique using secret bits
  - 2. codeword reversibility checking technique

Image repairing using secret bits

mapping function *H(S)*

$$H(S)=\begin{cases} 0\ or\ 1 & \cdots if\ LEN(S)=0 \\ INT(S)+2^{LEN(S)} & \cdots if\ LEN(S)>0 \end{cases} \qquad \overline{H}(I)=\begin{cases} EMPTY\ STRING\ \varepsilon & \cdots if\ I\le 1 \\ STR(I-2^{\lfloor \log_2 I\rfloor}, \lfloor \log_2 I \rfloor) & \cdots if\ I>1 \end{cases}$$

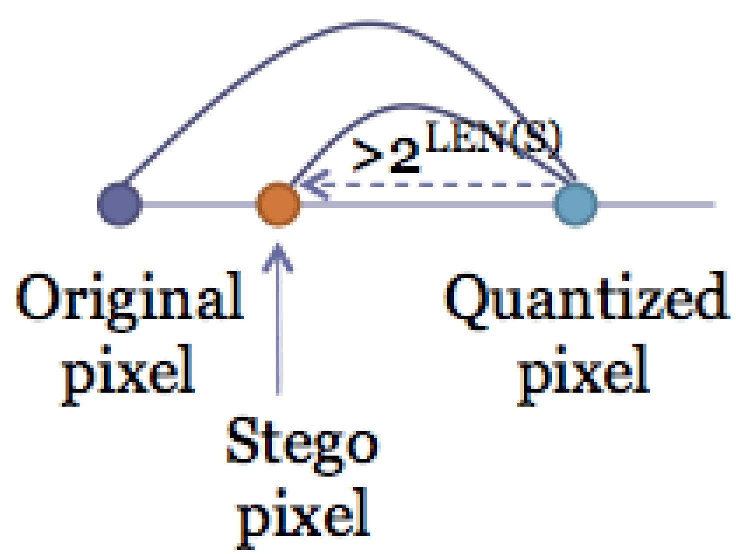

Two major points:
- Keep high visual quality
- Ensure the reversibility

(a) Cover image Lena

(b) SMVQ-compressed image Lena

(c) Stego-image Lena

(d) Face region of (a)

(e) Face region of (b)

(f) Face region of (c)

Fig. 7 The Lena image set: the cover image, the SMVQ-compressed image, and the stego-image, where the encoding uses the VQ codebook of 256 codewords and the state codebook size of 16 entries. (**a**) Cover image Lena. (**b**) SMVQ-compressed image Lena. (**c**) Stego-image Lena. (**d**) Face region of (**a**). (**e**) Face region of (**b**). (**f**) Face region of (**c**)

Table 3 The image quality in PSNR and the embedding capacity (EC) in bits of the stego-images, using different state codebooks and the codebook of 512 codewords

Image	Codebook size 512									
	8		16		64		128		256	
	PSNR	EC	PSNR	EC	PSNR	EC	PSNR	EC	PSNR	EC
Lena	36.87	339,033	38.68	272,799	41.35	214,260	42.15	201,031	42.51	194,884
Boat	36.73	365,403	38.18	318,438	40.29	261,791	41.09	247,141	41.54	239,249
F16	37.21	295,086	38.68	248,041	41.34	193,335	30.59	180,242	42.50	173,700
Baboon	34.63	645,814	35.22	599,943	36.47	535,441	37.10	512,438	37.53	498,377
Barbara	34.57	561,142	35.92	491,477	37.74	417,127	38.55	393,759	39.23	380,358
Bridge	34.49	667,267	35.58	609,000	37.19	533,110	37.68	512,755	37.97	502,237

科技醫療應用與安全

Q & A